The Thesis Committee for Sophia Katherine Beyer
Certifies that this is the approved version of the following thesis:

Matrix Metalloproteinase and Carbonic Anhydrase Detection Based on ^{19}F MRI and Fluorescence

APPROVED BY
SUPERVISING COMMITTEE:

Emily L. Que, Supervisor

Michael J. Rose

Matrix Metalloproteinase and Carbonic Anhydrase Detection Based on ^{19}F MRI and Fluorescence

by

Sophia Katherine Beyer

Thesis

Presented to the Faculty of the Graduate School of

The University of Texas at Austin

in Partial Fulfillment

of the Requirements

for the Degree of

Master of Arts

The University of Texas at Austin

December 2018

Acknowledgements

I would like to thank everyone in the Que lab for supporting me through graduate school and for helping make this thesis possible, particularly Radhika Mehta, Dr. Meng Yu, Kanchan Aggarwal, Da Xie, and Dr. Emily Que. I would also like to thank my family: Huntley, Jody, Gus, and Eva Beyer, for their endless love and support and for always being there for me.

Abstract

Matrix Metalloproteinase and Carbonic Anhydrase Detection Based on ^{19}F MRI and Fluorescence

Sophia Katherine Beyer, M.A.

The University of Texas at Austin, 2018

Supervisor: Emily Que

Zinc metalloproteins are heavily involved in a wide variety of human diseases,[1] such as rheumatoid arthritis, periodontitis, and cancer. Matrix metalloproteinase (MMP) and carbonic anhydrase (CA) are two zinc containing enzymes that are seen as attractive biomarkers for a multitude of pathological conditions, due to their overexpression in these diseases as well as their role in the spread and metastasis of cancer cells. Therefore, we focused on creating probes designed to track the location and relative concentration of matrix metalloproteinase and carbonic anhydrase through fluorescence and ^{19}F MRI. In the first project, an inhibitor and a set of fluorophores were synthesized to bind to MMPs and display a "turn on" signal. In the second project, a probe was designed to detect MMP activity through ^{19}F MRI. Finally, in the third project, a probe was created to detect CA activity via ^{19}F MRI. Here, we describe the synthesis and characterization of these probes and report preliminary UV and fluorescence response along with ^{19}F NMR T_1 and T_2 relaxivity.

Table of Contents

I. INTRODUCTION

Zinc is necessary for proper function and activity of a wide variety of enzymes.[2] With binding sites in tetrahedral or trigonal bipyramidal geometry, zinc is responsible for maintaining structure and stability while also participating in chemical catalysis.[2] One example of zinc containing enzymes are matrix metalloproteinases (MMPs). MMPs are zinc containing endopeptidases that degrade different components of the extracellular matrix.[3] These enzymes are expressed during tissue remodeling processes such as wound healing, uterine and mammary involution, and embryonic development.[3] However, they are also known to be overexpressed in multiple pathological conditions including rheumatoid arthritis, periodontitis, and tumor cell invasion and metastasis.[3] A second example of zinc containing enzymes is carbonic anhydrase (CA). CA is a lyase enzyme that catalyzes the reversible conversion of carbon dioxide to bicarbonate and it is responsible for transporting bicarbonate ions across membranes and blood during such processes as respiration.[4] CA is also known to be vital to the process of tumor progression and metastasis.[5] Therefore, we designed small molecule probes to track the location and relative concentration of these zinc metalloenzymes through fluorescence and ^{19}F MRI.

Fluorescence microscopy is the most widely used imaging technique in biological studies, particularly when monitoring cellular systems.[6] This is due to its high sensitivity, high spatiotemporal resolution, and simple experimental procedure.[6] To specifically target MMPs, fluorophores and an inhibitor with hydroxamic acid functionality were designed and synthesized (**Scheme 1**). Hydroxamic acids have been used as the zinc-binding group of choice for MMP targeting and inhibition.[7] The fluorophores were based off of a known compound, N,N-dimethylaminopthalimide (DMAP)[8] that is not fluorescent in aqueous environments and fluorescent in hydrophobic environments including enzyme active sites[4] (**Figure 1A**). The

fluorescent probes were synthesized with different linker lengths in order to compare binding efficiency.

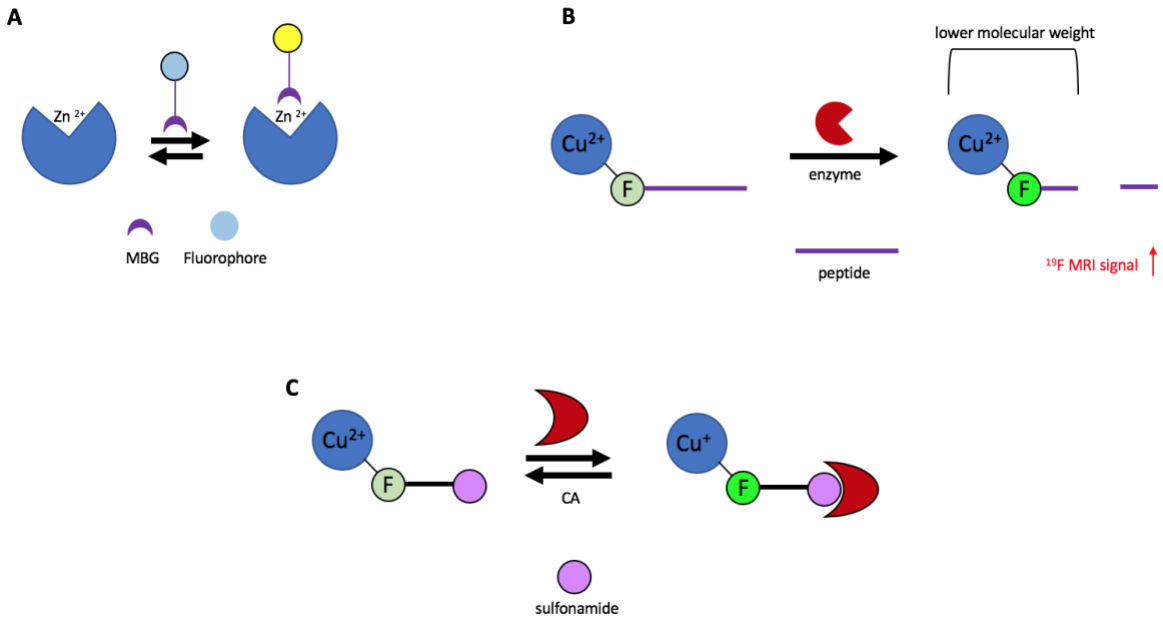

Figure 1: (A) Representation of fluorescent "turn on" response of probes **5.1** – **5.4** in the hydrophobic environment of the MMP active site. MBG represents the metal binding group. (B) Design strategy for probe **25**, which will be cleaved by MMP creating two fractions of lower molecular mass resulting in an increased ^{19}F MRI signal. (C) Design strategy for hypoxia-induced Cu^{2+} based probe **38**, which results in an increased ^{19}F MRI signal when bound to CA.

In addition to fluorescence, we also used ^{19}F magnetic resonance imaging (MRI) as a method to track MMP location and activity (**Scheme 2**). MRI is a noninvasive technique that provides important medical information on deep tissues that cannot be acquired through other methods.[9] Due to its visualization of deep regions of human and animal bodies, MRI is one of the most successful imaging techniques for diagnosis.[6] This probe was designed with three basic components: a metal coordination site, a fluorine tag, and a peptide sequence that is specifically cleaved by MMPs. The metal coordination serves as a paramagnetic imaging reporter.[10] The intact probe will be silent to magnetic resonance (MR) imaging until cleaved by MMP, when the probe

will be altered into a fragment with a different relaxivity, thus creating a high contrast enhancement.[10] When the probe gets cleaved, this results in two smaller fragments. This decrease in molecular mass is expected to cause a significant decrease in the ^{19}F relaxation rate, creating a signal in MRI.[11] We chose to use a fluorine tag due to the preferable MR properties of the ^{19}F nucleus and minimal signal in the human body, as compared to ^{1}H MR imaging.[12]

A fluorine tag was also used in our final probe, designed to track CA location through ^{19}F MRI (**Scheme 3**). This probe was designed with a metal chelator, a fluorine tag, a PEG linker, and a sulfonamide functionality. The sulfonamide group was chosen as a selective target for CA, due to its significant CA binding ability.[13] Sulfonamides bind in a tetrahedral geometry of the Zn(II) ion in a deprotonated state, with the nitrogen atom coordinating to the zinc.[14] The PEG linker connects the sulfonamide group to the fluorine tag, which is then connected to the Cu(II) coordination complex 1,4,7-triazacyclononane (TACN). CA (especially CAIX) is selectively expressed in hypoxic tumors and promotes tumor cell survival and invasion in hypoxic microenvironments.[5] These probes should function via signal accumulation on cells that over express CAIX. PEG linkers of different lengths were synthesized to determine optimal distance between the sulfonamide moiety and the bulky TACN group. The synthesis and characterization of these metalloenzyme probes is discussed here.

II. RESULTS AND DISCUSSION

Chapter 1: MMP Targeted Inhibitor and Fluorophores

To construct fluorophores specific for MMPs, four probes containing varying linker lengths were synthesized. A known inhibitor for MMP was also synthesized as a control molecule (**Scheme 1**). Detailed synthesis of these probes can be found in the "Materials and Methods" section.

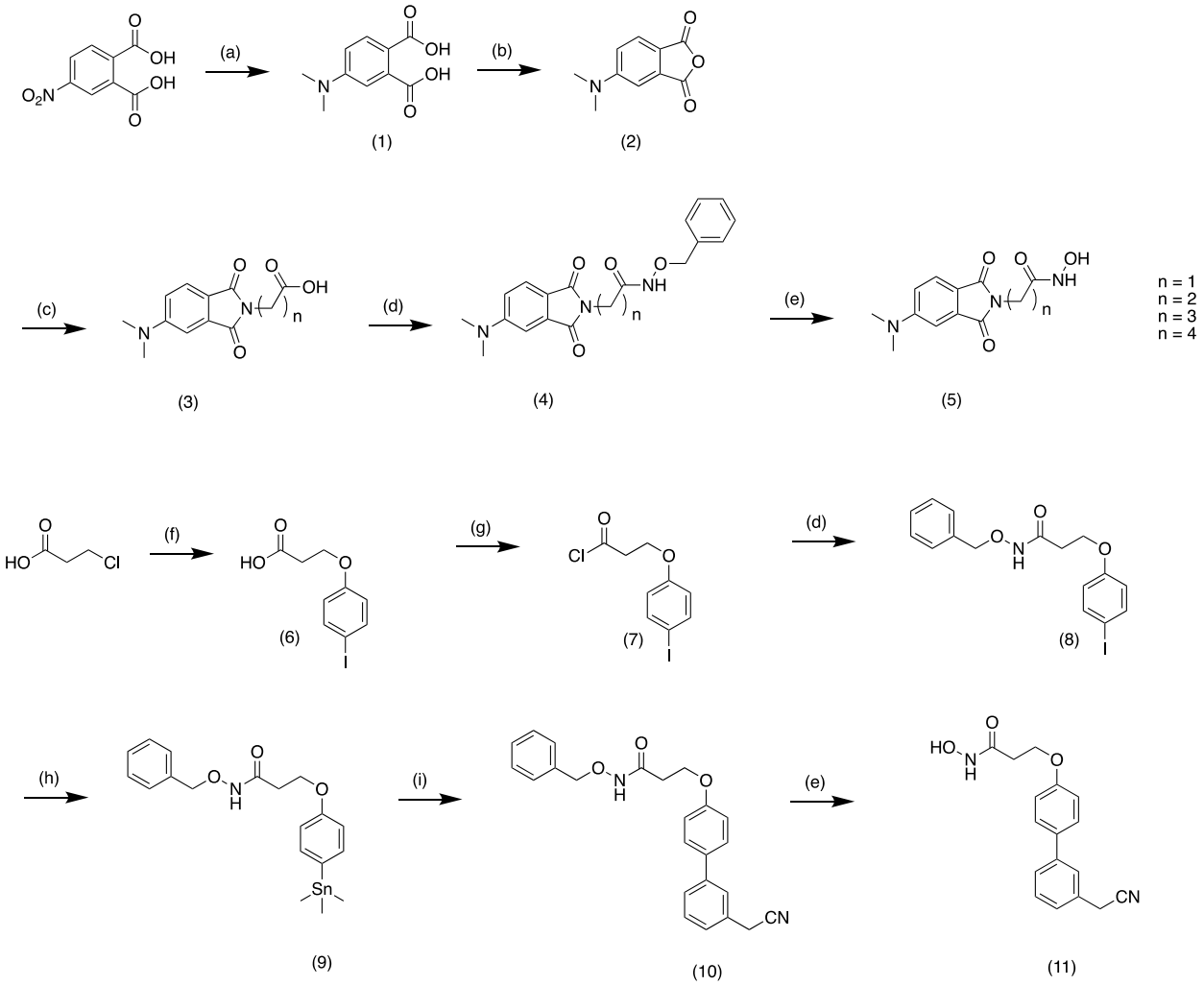

Scheme 1. Conditions: (a) HCHO, H_2, Pd/C, MeOH, O.N. (b) 120 °C, O.N. (c) glycine (n=1), gamma-aminobutyric acid (n=2), 5-aminovaleric acid (n=4), TEA, toluene, reflux (d) O-benzylhydroxylamine, EDC, DIPEA, $CHCl_3$, O.N. (e) H_2, Pd/C, MeOH, O.N. (f) 4-iodophenol, NaOH, 40 °C (g) $SOCl_2$, reflux (h) hexamethyldistannane, $Pd(PPh_3)_4$, toluene, reflux (i) 3-iodophenylacetonitrile, $Pd(PPh_3)_4$, toluene, reflux

Once the four fluorophores were synthesized (compounds **5.1**, **5.2**, **5.3**, and **5.4**, n = 1, 2, 3, and 4, respectively), solvent studies were performed. The UV-Vis absorbance and fluorescence intensity were measured for each fluorophore, at concentrations of 1 – 10 µM. Probe **5.2** had a greater absorbance in the non-polar solvents, as expected. However, probe **5.1** showed a larger absorbance in chloroform and methanol, probe **5.3** had the highest absorbance in DMSO, and probe **5.4** had the highest absorbance in chloroform. Overall, toluene, chloroform, and DMSO provided larger fluorophore absorbance values when compared to methanol and water. **Figure 2** provides a comparison of the molar absorptivity values of each of the four fluorophores in the five solvents tested. **Figure 3** and **Figure 4** show representative absorbance and fluorescence spectra (respectively), one for each fluorophore (2 µM), in the different solvents. **Table 1** includes all of the numerical data collected during the solvent study, including the wavelength of maximum absorbance, the molar absorptivity, and the emission wavelengths for the four fluorophores in the five tested solvents. The excitation wavelength was the same as the λ_{max}. There is a bathochromic shift in λ_{max} and λ_{em} for all molecules upon going from non-polar to more polar solvents due to solvent relaxation.[16] More notably, the shift in wavelength is accompanied by a decrease in fluorescence intensity in polar solvents, which is due to a twisted intramolecular charge transfer (TICT) state.[17, 18]

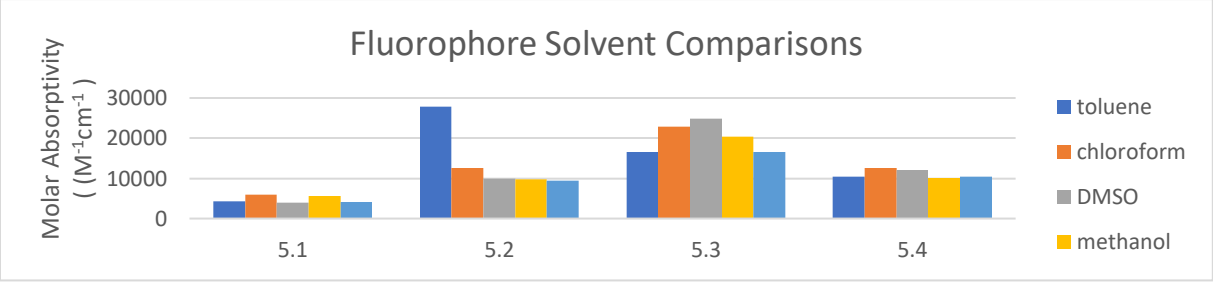

Figure 2: Solvent polarity study with fluorophores. Each fluorophore absorbance was monitored in five different solvents: toluene, chloroform, DMSO, methanol, and water (in order of increasing polarity).

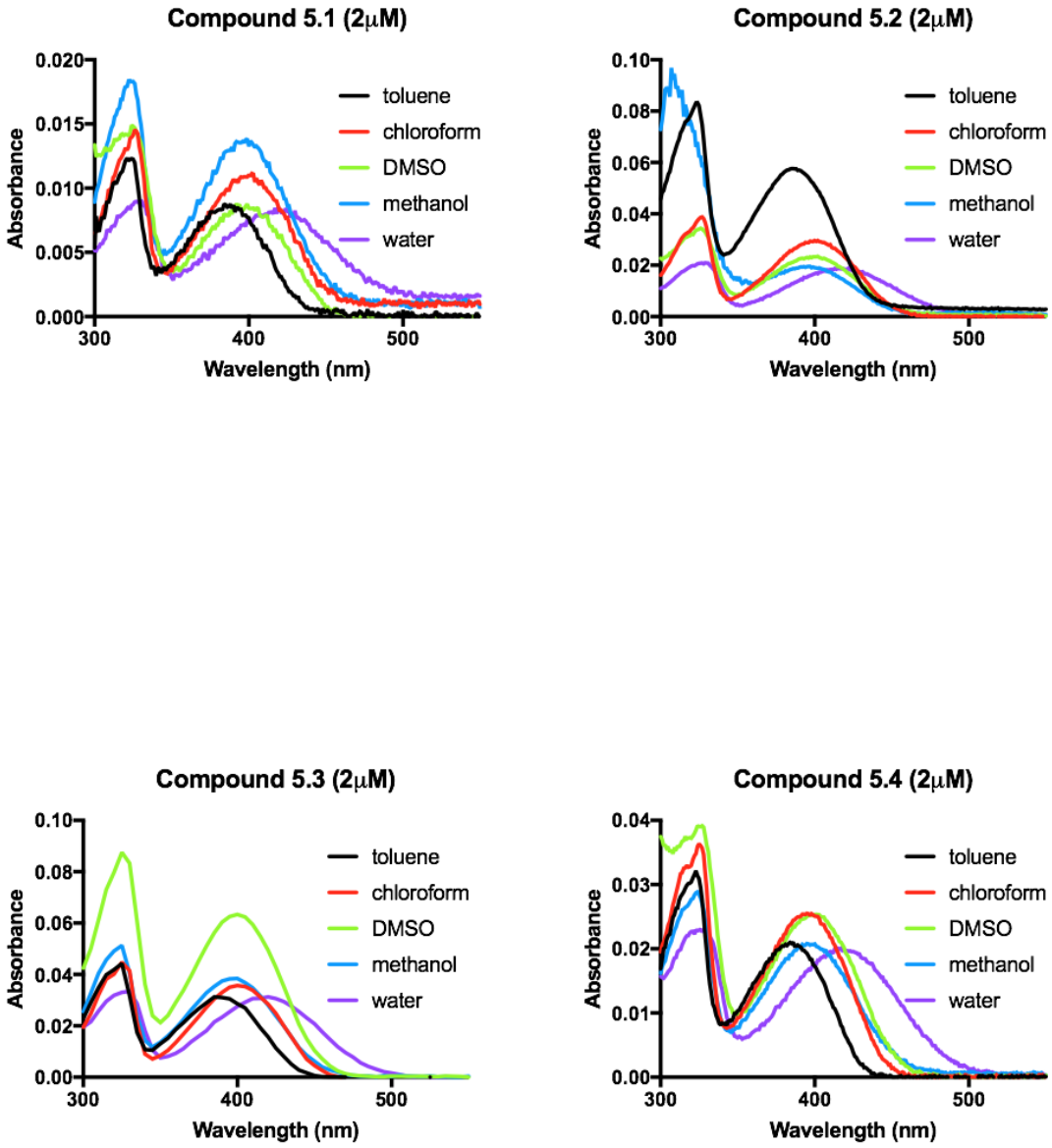

Figure 3: Graphs showing fluorophore UV-Vis absorbances in toluene, chloroform, DMSO, methanol, and water to compare absorbance values in different solvent polarities. Each fluorophore was measured at a concentration of 2 μM in solution and the measurements were taken at room temperature.

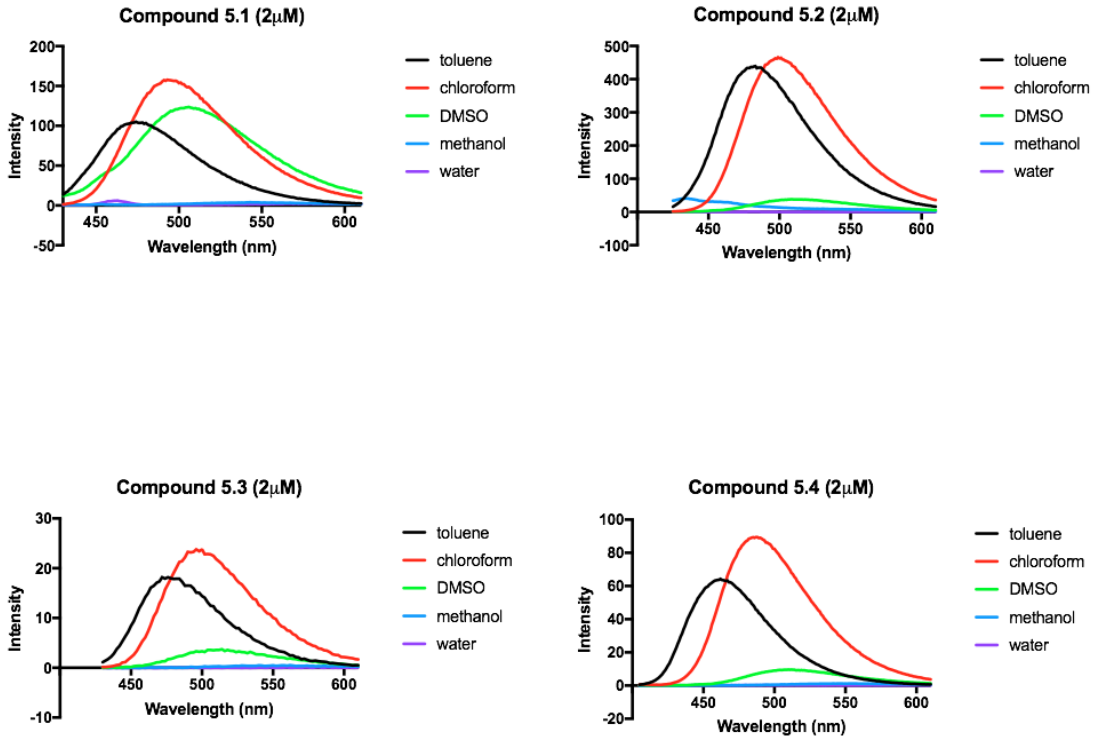

Figure 4: Graphs showing fluorophore fluorescence intensities in toluene, chloroform, DMSO, methanol, and water to compare absorbance values in different solvent polarities. Each fluorophore was measured at a concentration of 2 μM in solution and the measurements were taken at room temperature.

Probe		toluene	chloroform	DMSO	methanol	water
	λ_{max} (nm)	384	400	400	395	418
5.1	ε ($M^{-1}cm^{-1}$)	4320	5895	3904	5654	4094
	λ_{em} (nm)	475	495	508	545	590
	λ_{max} (nm)	386	400	400	395	418
5.2	ε ($M^{-1}cm^{-1}$)	27913	12570	9933	9725	9394
	λ_{em} (nm)	484	500	513	550	595
	λ_{max} (nm)	390	400	400	400	420
5.3	ε ($M^{-1}cm^{-1}$)	16513	22863	24900	20384	16635
	λ_{em} (nm)	480	500	515	550	600
	λ_{max} (nm)	384	396	400	400	420
5.4	ε ($M^{-1}cm^{-1}$)	10448	12514	12061	10057	10451
	λ_{em} (nm)	465	487	510	550	595

Table 1: Summation of solvent study data, showing the wavelength of maximum absorbance, the molar absorptivity, and the excitation and emission wavelengths for the four fluorophores in the five tested solvents: toluene, chloroform, DMSO, methanol, and water.

Following the solvent studies, fluorescence of the four fluorophores was monitored as bovine CA (bCA) was introduced to the system. The fluorophores were tested with bCA while awaiting the arrival of the MMP enzyme, as well as a means to become familiarized with the UV and fluorimeter instrumentation and techniques. An interaction of the fluorophores with bCA was not expected and is not seen in **Figure 5**. The fluorescence intensity was monitored while different concentrations of fluorophore and bCA were added to the cuvette. **Figure 5A-C** show the fluorescence spectra for probe **5.1-5.3** in the absence (purple) and presence of 1 equiv bCA (red). The graphs show no increase in fluorescence in the presence of bCA that suggests the lack of interaction between the probe and the protein. A final test was performed with the fluorophore concentrations being significantly higher than the bCA concentrations (**Figure 5D**). Results were as expected; the higher equivalents of probe added to bCA additions did not alter the fluorescence of the fluorophores.

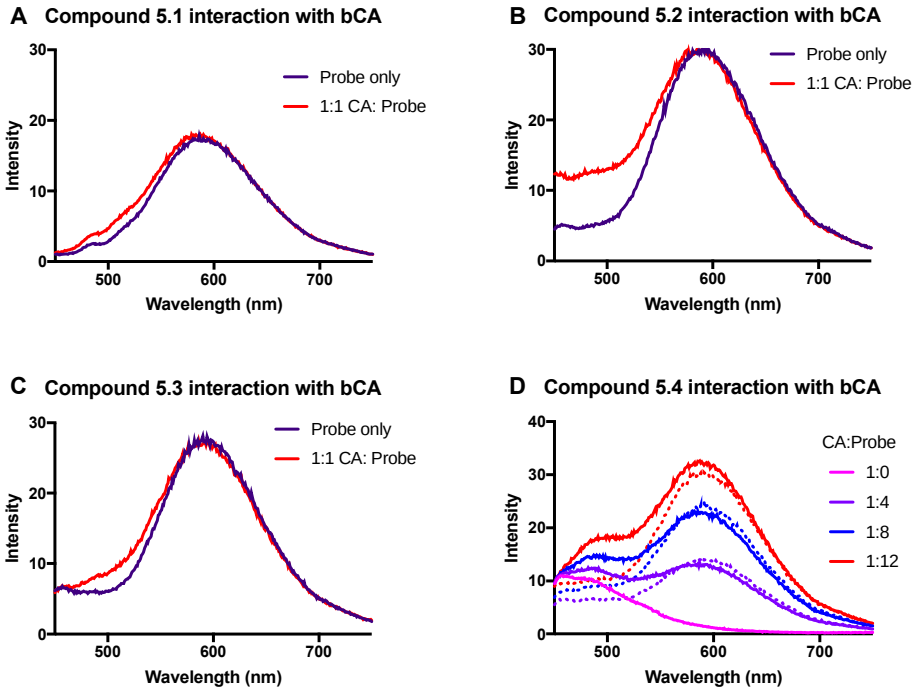

Figure 5: (A-C) Fluorescence spectra of probes **5.1** to **5.3** (5 µM) in the absence (purple) and presence (red) of 1 equiv. bCA in HEPES buffer (pH 7.2) at room temperature. (D) Fluorescence spectra of 5 µM bCA with higher equivalence of probe **5.4** (4, 8, and 12 equivalents) to study binding with CA. The spectra for probe **5.4** only are shown as dotted lines.

To further test the lack of binding and interaction of the fluorophores with bCA, we performed the 4-nitrophenylacetate (NPA) assay. NPA assay tests the activity of bCA by following the hydrolysis of 4-nitrophenylacetate to 4-nitrophenolate ion that absorbs at 400nm. NPA assay performed with compounds **5.1** and **5.4** (**Figure 6)** showed neither of the compounds decreased the activity of bCA that supports the fact that these molecules indeed do not inhibit CA. There were some unexpected results however, in the fact that they increased bCA activity to greater than 100% (compound **5.1** increased to 123% bCA activity and compound **5.4** increased to 119% bCA activity).

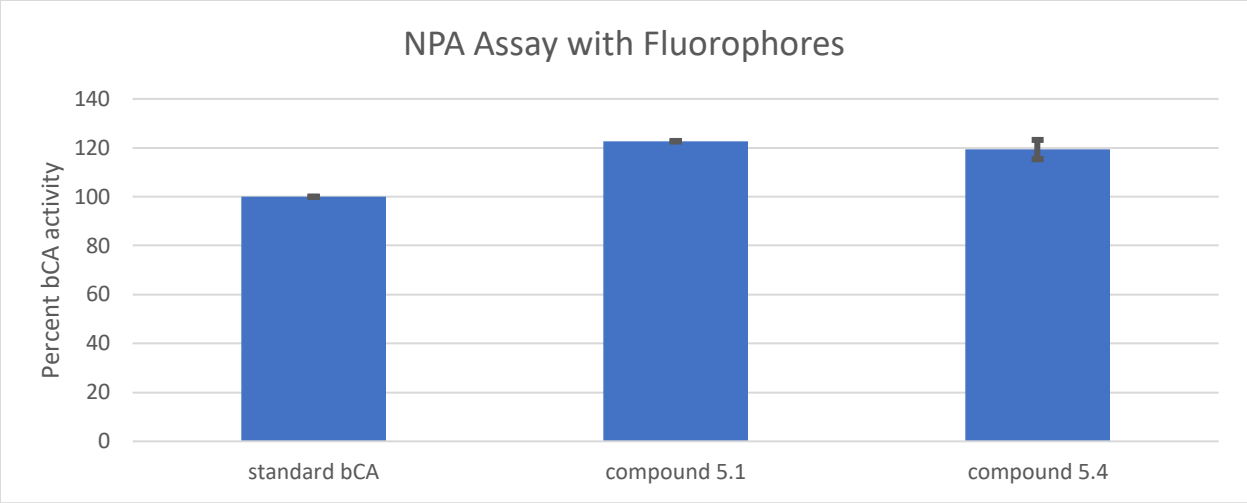

Figure 6: NPA assay with compounds **5.1** and **5.4**. These assays were performed in 50mM HEPES buffer with 100 mM KNO_3, pH 7.2 at room temperature.

Chapter 2: MMP Detection Through ^{19}F MRI

A probe that detects the presence of MMP upregulation via ^{19}F MRI was synthesized, along with two control probes, one without the TACN functionality and one with a "pre-cleaved" amino acid linker (**Scheme 2**). The idea behind this design was to have a probe silent to MR initially, until the peptide sequence is cleaved by MMP at which point the molecular mass of the probe will significantly decrease, causing a decrease in ^{19}F relaxation rate, resulting in a MR signal.[10] Cu^{2+} will be used as the paramagnetic reporter. The synthetic scheme is shown below. Detailed synthesis of these probes can be found in the "Materials and Methods" section.

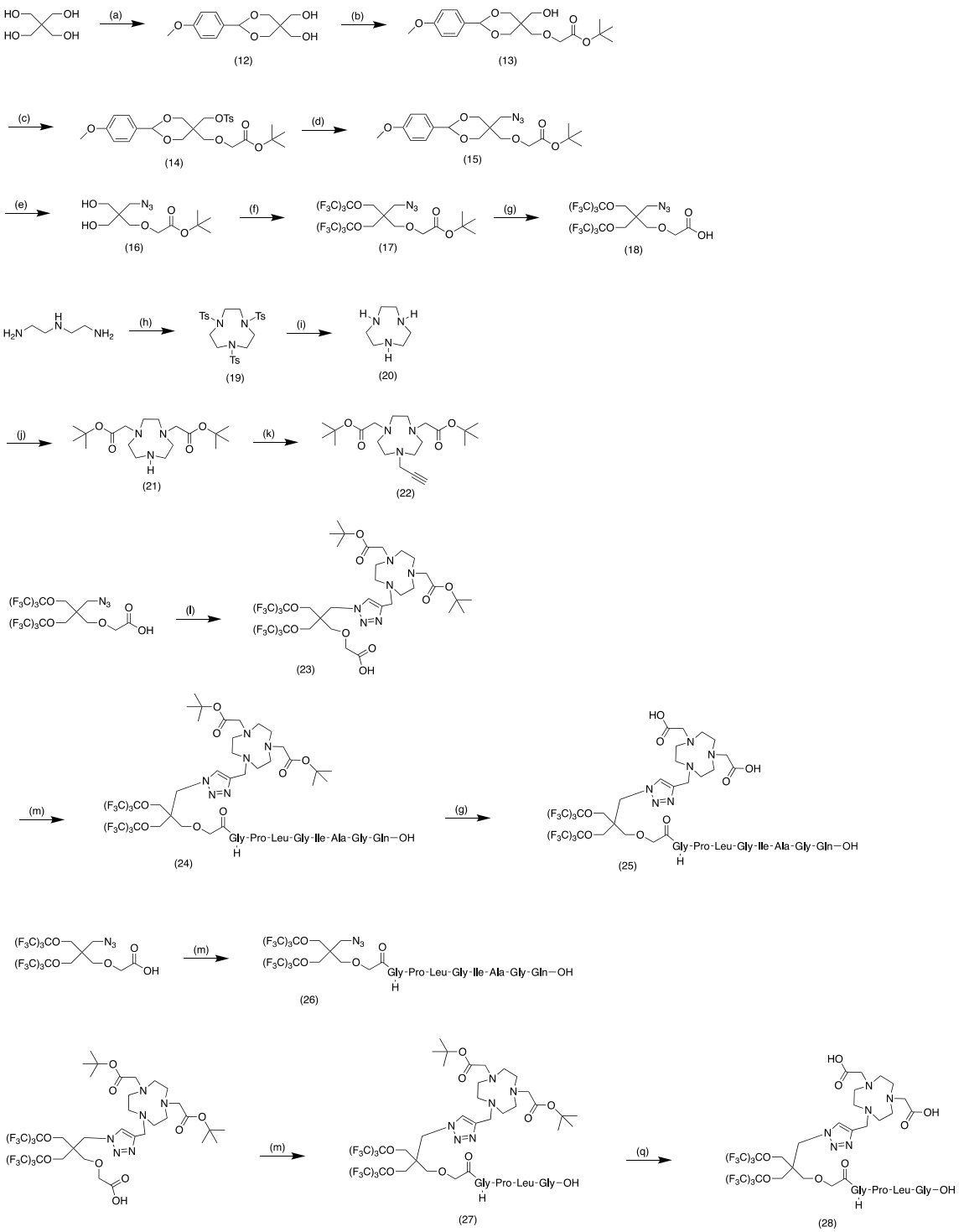

Scheme 2. Conditions: (a) P-anisaldehyde, HCl, H_2O (b) tert-butyl 2-bromoacetate, KOtBu, THF/DMF, 45 °C (c) TsCl, DMAP, 0 °C, DCM (d) NaN3, DMF (e) HOAc, H_2O, 40 °C (f) F_9OH, PPh_3, DIAD, THF (g) TIS, TFA, H_2O (h) TsCl, 1,2-dibromoethane, K_2CO_3, H_2O, PhMe, NaOH, Bn_4NBr (i) NaOH (j) bromoethylacetate, $NaHCO_3$, $CHCl_3$ (k) 3-bromoprop-1-yne, K_2CO_3, ACN (l) **22**, ascorbic acid, copper sulfate, degassed H_2O, DCM (m) peptide (prepared via peptide synthesizer), DIPEA, HATU, DMF

The synthesized molecules were characterized via NMR. The T_1 and T_2 data is summarized in **Table 2** below. T_1 and T_2 data was first gathered for compound **26** on the 60 MHz NMR. The compound was not completely soluble in 1 mL D_2O, so 1 mL ACN was added; thus the NMR data was collected in a solution of 1:1 D_2O:ACN. The T_1 and T_2 values were determined to be 1.44 seconds and 1.437 seconds, respectively, which resulted in sharp peaks. The ^{19}F NMR spectrum of this compound can be seen below (**Figure 7**). Next, T_1 and T_2 data was collected for compound **25**, which was soluble in 100% D_2O. The T_1 analysis showed very small, broad peaks on both the 60 MHz NMR and the 400 MHz, which suggested aggregation. This result lead to DLS and DOSY NMR analysis, both of which confirmed the presence of aggregates. Compound **25** was then dissolved in 600 µL of 100 mM ammonium acetate buffer (pH 5.05), in order to have a better understanding of peptide charge while performing these experiments. 120 µL of D_2O (20%) was added to the solution to allow for further NMR analysis. The 60 MHz NMR showed T_1 and T_2 values of 122 ms and 19.2 ms respectively; since these values are significantly different from one another, the peaks were very broad. The same analysis was performed on the 400 MHz NMR, which resulted in T_1 and T_2 values of 253 ms and 6.75 ms, respectively. This data supports the significant difference between the T_1 and T_2 values seen on the 60 MHz NMR. The ^{19}F NMR spectrum for compound **25** can be seen below (**Figure 8**). It is possible that compound **25** experiences temperature dependence; perhaps the compounds in solution are arranging in such a way that beta sheets are forming around the fluorine groups, quenching any possible signal. NMR analysis should be performed at different temperatures. The same T_1/T_2 analysis was then performed on compound **28**, in 80:20 100 mM ammonium acetate buffer (pH 5.05):D_2O. The 60 MHz NMR provided T_1 and T_2 values of 245.5 ms and 12.79 ms, respectively, while the 400 MHz NMR reported T_1 and T_2 values of 248.75 ms and 13.125 ms, respectively. The two NMR

instruments showed the same significant difference between the T_1 and T_2 values and thus both conveyed broad peaks during this analysis. Once again, this lead to the question of aggregation. Further studies need to be performed to conclude how the molecules are interacting intramolecularly and intermolecularly in solution. **Figures 9 – 12** below show the T_1 and T_2 correlation analysis performed on 60 MHz NMR in ammonium acetate buffer (with 20% D_2O) for compounds **25** and **28**.

Compound	Solvent	Instrument	T_1 (ms)	T_2 (ms)
26	50:50 ACN : D_2O	60 MHz	1440	1437
25	100% D_2O	60 MHz	too broad	too broad
25	80:20 ammonium acetate buffer : D_2O	60 MHz	122	19.2
25	80:20 ammonium acetate buffer : D_2O	400 MHz	253	6.75
28	80:20 ammonium acetate buffer : D_2O	60 MHz	75.705	12.79 34.42
28	80:20 ammonium acetate buffer : D_2O	400 MHz	248.75	13.125

Table 2: Table summarizing the T_1/T_2 analysis of compounds **25**, **26**, and **28**. These values were collected on either a 60 MHz benchtop NMR or a 400 MHz NMR, at room temperature.

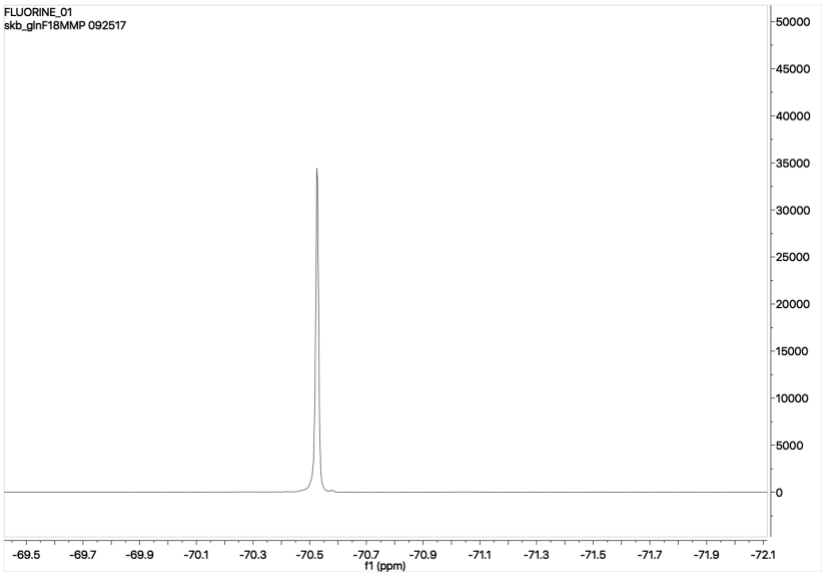

Figure 7: ^{19}F NMR of compound **26** in deuterium oxide at room temperature at 400 MHz.

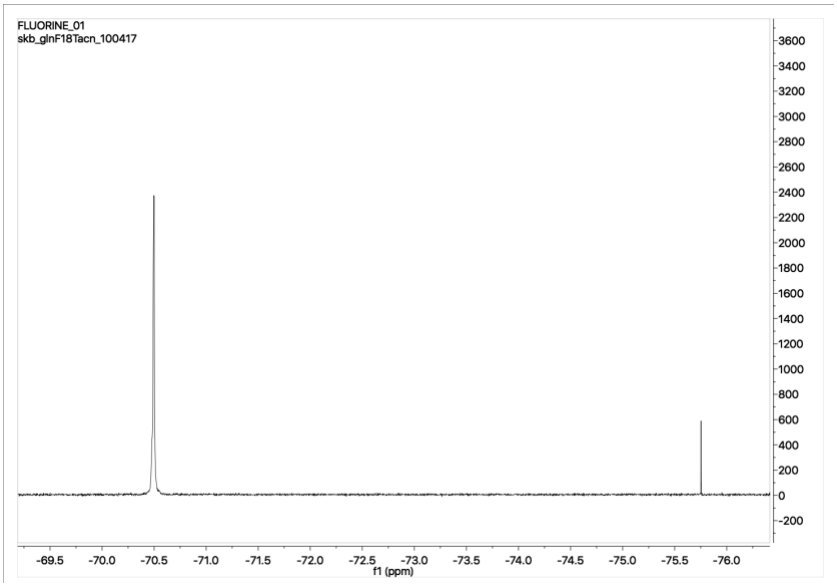

Figure 8: ^{19}F NMR of compound **25** in deuterium oxide at room temperature at 400 MHz.

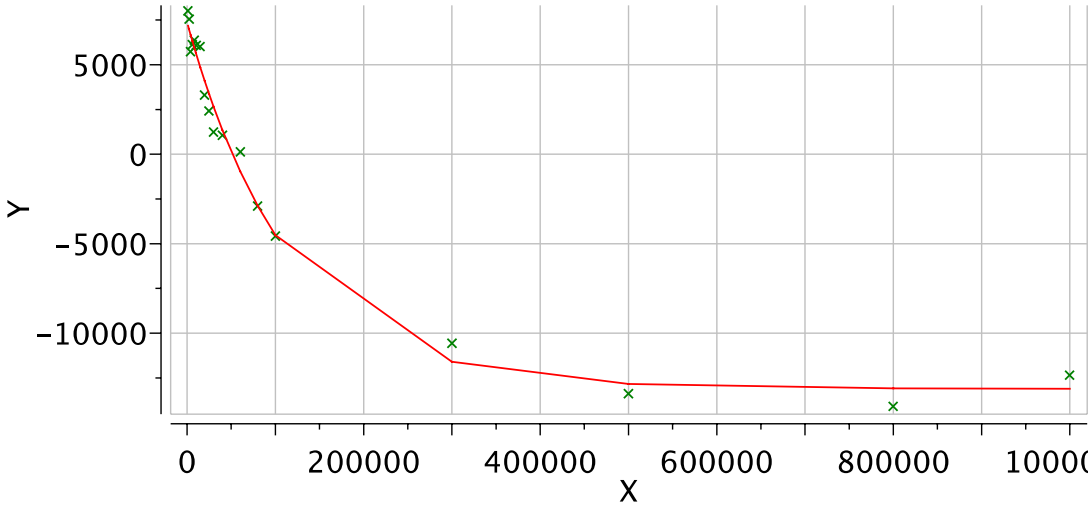

Figure 9: T_1 NMR analysis of compound **25**, performed in ammonium acetate buffer on the 60 MHz benchtop NMR.

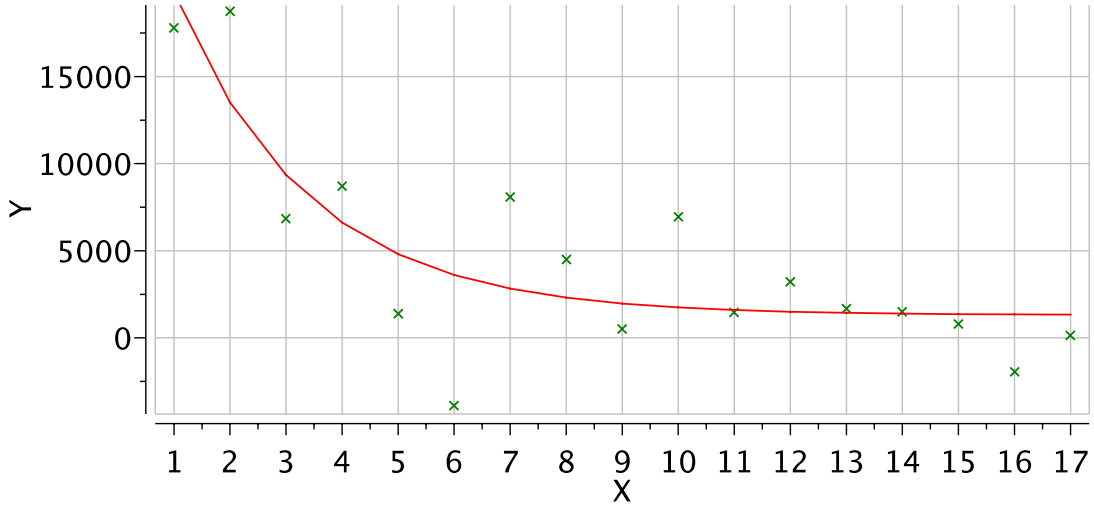

Figure 10: T_2 NMR analysis of compound **25**, performed in ammonium acetate buffer on the 60 MHz benchtop NMR.

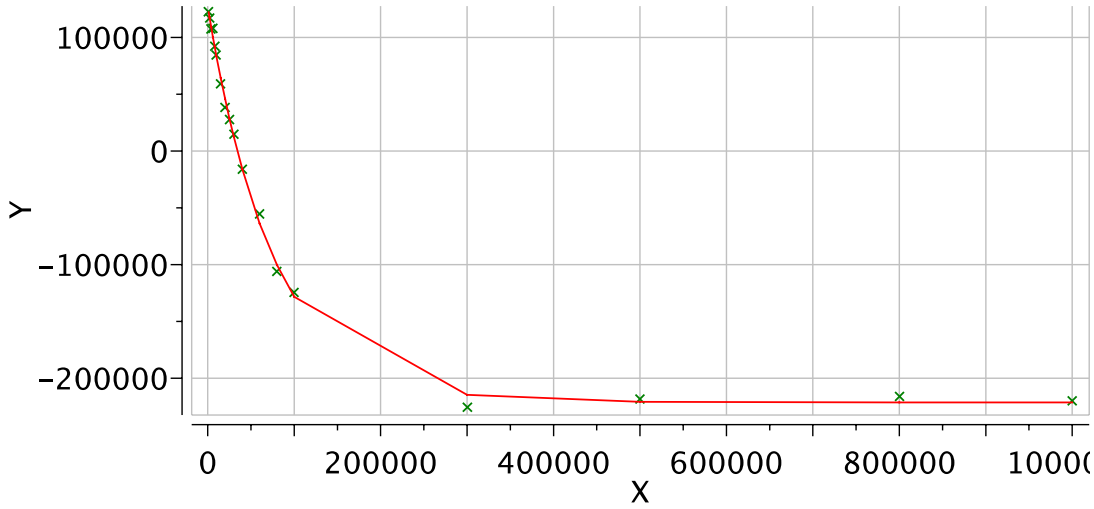

Figure 11: T_1 NMR analysis of compound **28**, performed in ammonium acetate buffer on the 60 MHz benchtop NMR.

Figure 12: T_2 NMR analysis of compound **28**, performed in ammonium acetate buffer on the 60 MHz benchtop NMR.

Chapter 3: CA Detection Through ^{19}F MRI

Two preliminary probes of varying linker lengths were built to detect CA upregulation through ^{19}F MRI (**Scheme 3**). The purpose of the sulfonamide functionality is to selectively bind the probe to CA and allow for probe accumulation at the tumor site.[13] Detailed synthesis of these probes can be found in the "Materials and Methods" section.

There was a major issue encountered when performing the synthesis of compounds **33** and **36**: the coupling of compound **23** to compounds **32** and **35** was not successful through the use of HATU as a coupling agent (determined by the 8% yield). Mass spectroscopy revealed that the majority of compound **23** was left unreacted, even after the reaction was stirred for two days. This situation was remedied by replacing HATU with PyBOP (with all other conditions left the same). After this change was made, the yield was significantly increase to 48%.

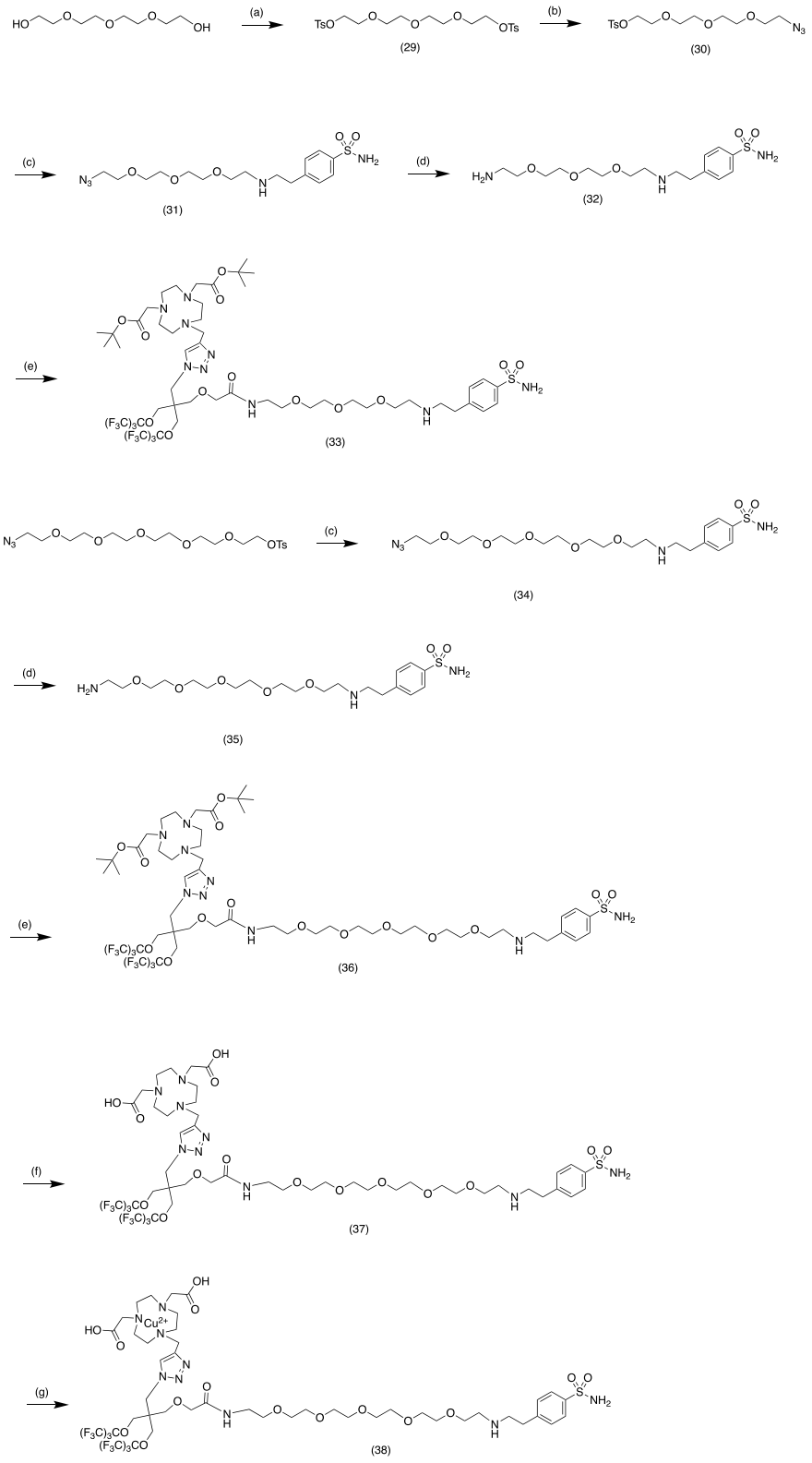

Scheme 3. Conditions: (a) TEA, TsCl, DCM (b) NaN_3, EtOH, 80 °C (c) 4-(2-aminoethyl)benzenesulfonamide, K_2CO_3, DMF, 80 °C (d) H_2, Pd/C, MeOH (e) **2b**, PyBOP, DIPEA, DMF (f) TIS, TFA, H_2O (g) copper acetate, H_2O

To study the interaction of compound **33** with carbonic anhydrase, an NPA assay was performed (**Figure 13A**). The bCA and compound **33** concentrations were both 2 µM. The NPA was in excess (125 µM). The compound did not show significant binding, decreasing the bCA activity to only 86%. This data was reproducible. Following this, a study was done to compare bCA activity with different ratios of compound **33** to bCA (**Figure 13B**). The results were inconclusive, which suggested that the compound is slower to bind to bCA than NPA. Therefore, these assays were followed up by NPA assays performed after an incubation period, where compound **33** was incubated with bCA at room temperature for 30 minutes and 60 minutes before NPA was added (**Figures 14A and 14B**, respectively). The 30 minute and 60 minute incubation periods resulted in bCA activity decreasing to 70% and 85%, respectively.

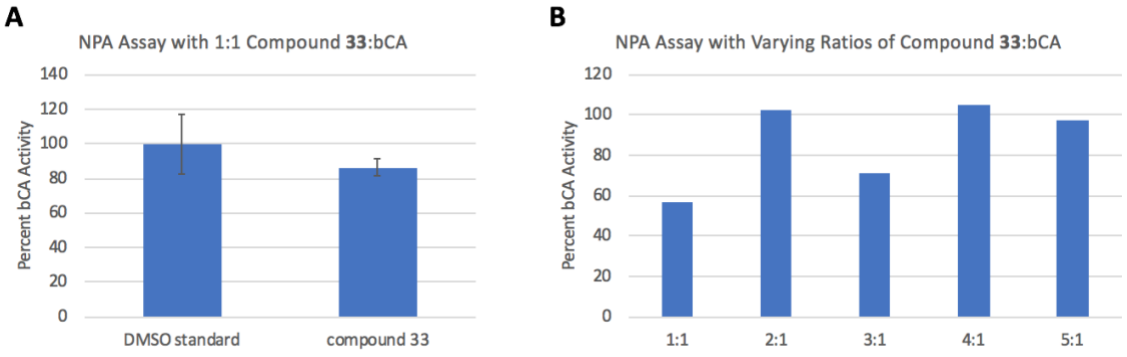

Figure 13: (A) NPA assay with compound **33** performed in 50mM HEPES buffer with 100 mM KNO_3, pH 7.2 at room temperature. (B) NPA assay performed with varying ratios of bCA to compound **33**, performed in 50mM HEPES buffer with 100 mM KNO_3, pH 7.2 at room temperature.

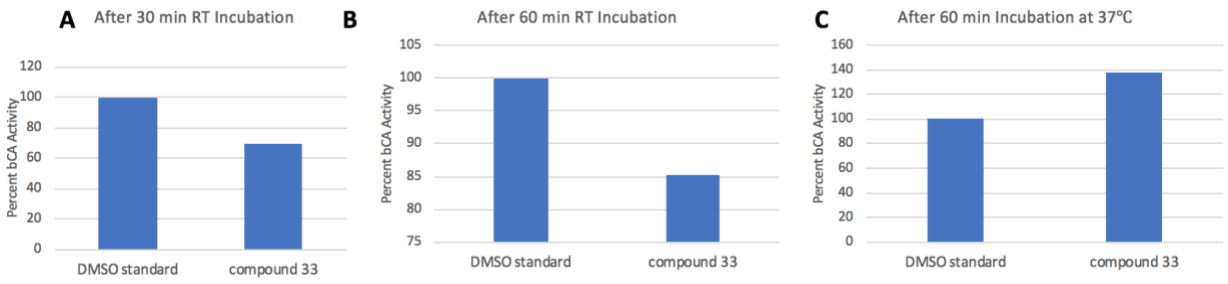

Figure 14: (A) NPA assay after 30 minute room temperature incubation period of compound **33** and bCA, performed in 50mM HEPES buffer with 100 mM KNO_3, pH 7.2. (B) NPA assay after 60 minute room temperature incubation period of compound **33** and bCA, performed in 50mM HEPES buffer with 100 mM KNO_3, pH 7.2. (C) NPA assay after 60 minute incubation period of compound **33** and bCA at 37 °C, performed in 50mM HEPES buffer with 100 mM KNO_3, pH 7.2.

Due to the fact that incubating the probe with bCA before the NPA assay was not showing a significant decrease in bCA activity, incubation at 37 °C for 60 minutes was also explored (**Figure 14C**). These results were not as expected, as the bCA activity increased to 138%. After these results, the binding was analyzed through a 5-(dimethylamino)naphthalene-1-sulfonamide (DNSA) assay. DNSA is not fluorescent on its own but forms a highly fluorescent complex with CA and binds to CA well due to its sulfonamide functionality.[19] Therefore, fluorescence was monitored to detect DNSA binding to the CA active site. After the DNSA was bound to CA, our probes were added to the solution and a decrease in fluorescence was expected due to the probes binding stronger to CA than DNSA, thus kicking DNSA out of the CA active site and becoming non-fluorescent. **Figure 15** shows standard DNSA additions to a solution of HEPES (1 mL) and bCA (0.25 µM); the additions were made in 0.25 µM increments, for a total concentration of 2.5 µM. Once the DNSA was added, compound **33** was added to the solution in 0.05 µM increments (**Figure 16**). The total probe concentration reached 0.5 µM, 2 equivalents as compared to the bCA. The results were as expected, as the tryptophan fluorescence increased (340 nm) while the DNSA fluorescence decreased (470 nm). This assay showed some binding of the probe to bCA, however

not in a significant quantity; the DNSA intensity decreased from 134 a.u. to 115 a.u. A second DNSA trial was performed on compound **33** (**Figure 17**). This trial was a repeat of trial 1, however this time 12 equivalents of compound **33** were added, for a total probe concentration of 3 µM. This trial provided different results from the previous trial, with the DNSA intensity decreasing with the additions of probe (124 a.u. to 40 a.u.), showing probe binding to bCA. The results of these two trials are different due to the change in probe equivalents added (2 equivalents versus 12 equivalents); these results show that a significant concentration of compound **33** is necessary in order to see binding to bCA.

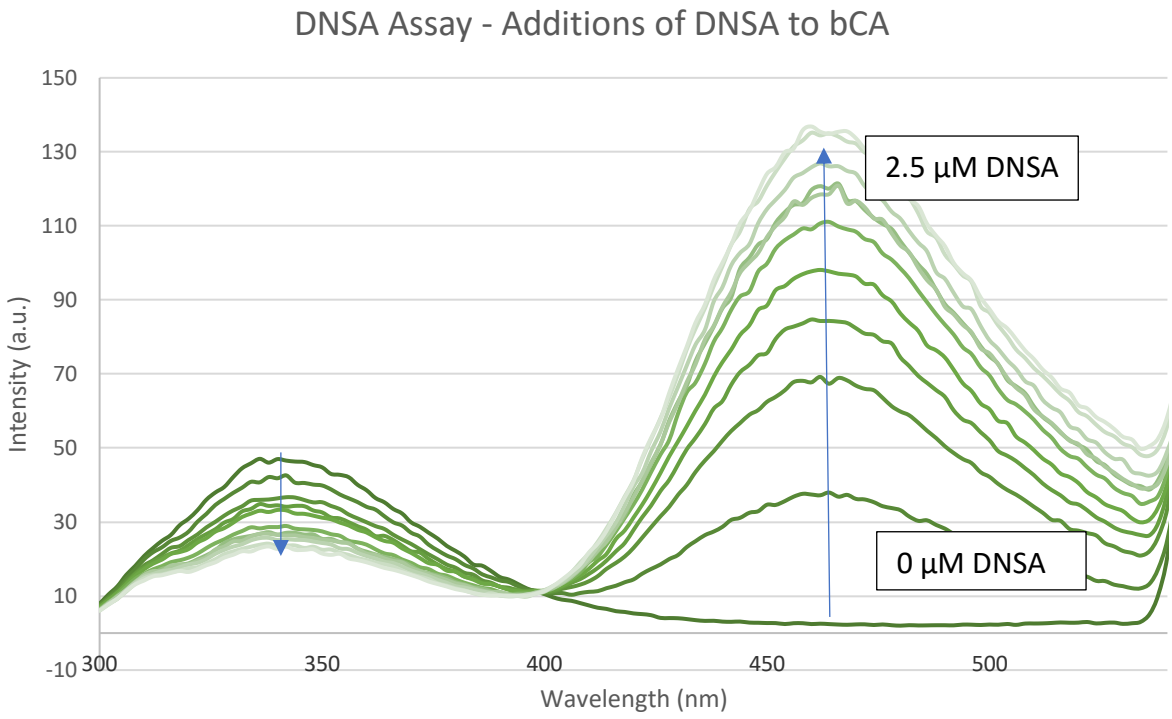

Figure 15: Standard DNSA additions to bCA in 50mM HEPES buffer with 100 mM KNO_3, pH 7.2, at room temperature. Concentration of DNSA increased from 0 µM to 2.5 µM.

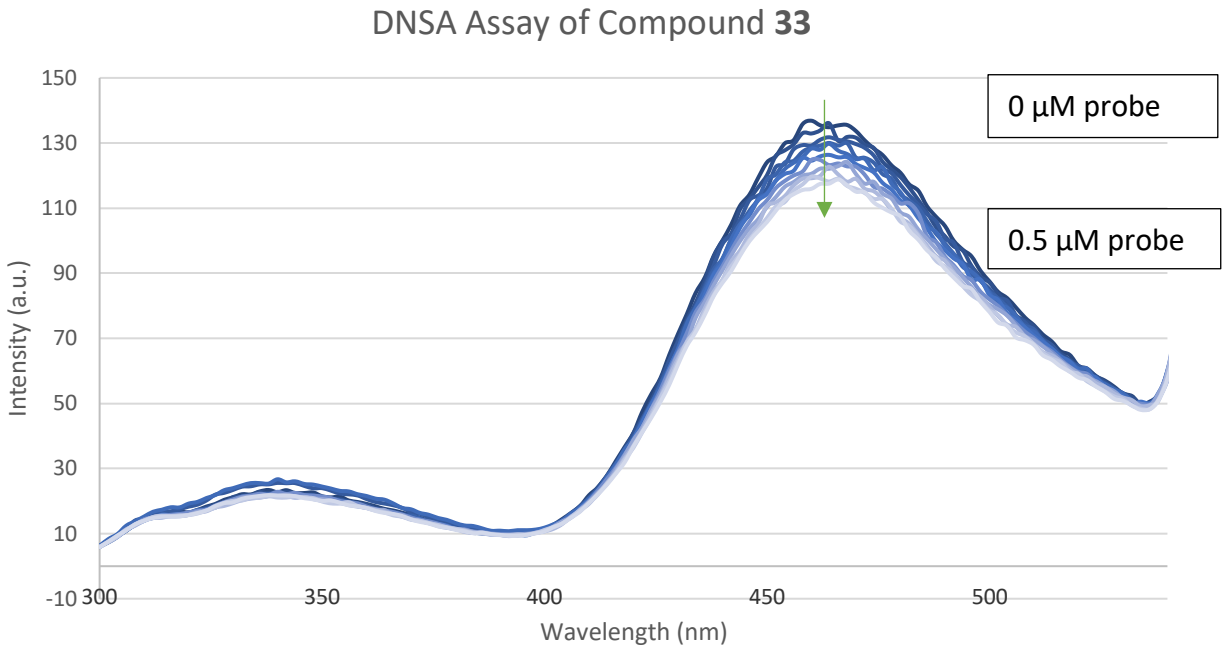

Figure 16: DNSA assay with compound **33** in 50mM HEPES buffer with 100 mM KNO_3, pH 7.2, at room temperature. Concentration of probe increased from 0 µM to 0.5 µM. Concentration of DNSA was 2.5 µM.

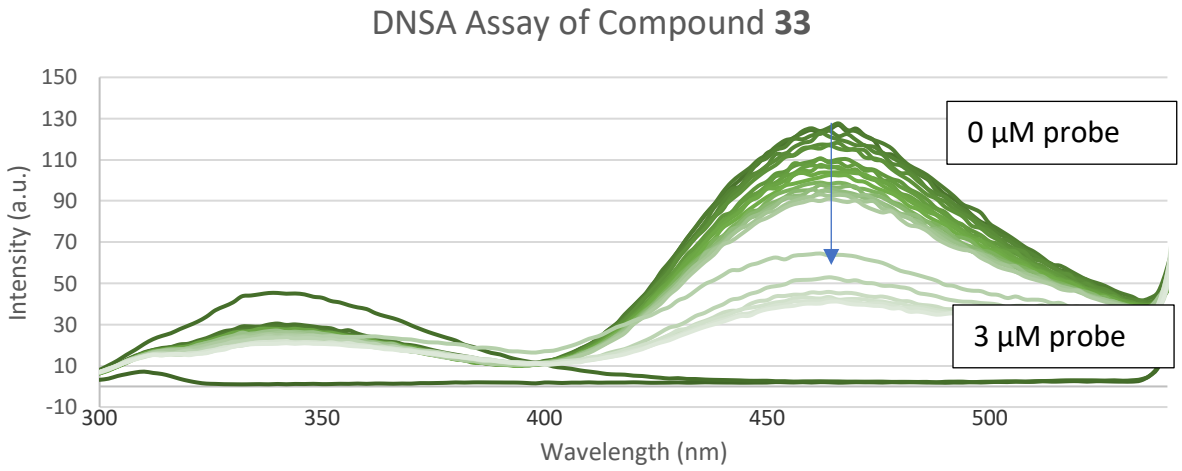

Figure 17: DNSA assay with compound **33** in 50mM HEPES buffer with 100 mM KNO_3, pH 7.2, at room temperature. Concentration of probe increased from 0 µM to 3 µM. Concentration of DNSA was 2.5 µM.

It was speculated that sterics were contributing to the poor binding of compound **33** to bCA, due to the bulky TACN functional group. This was when compound **37** was synthesized; it

was hypothesized that a longer PEG chain would reduce the steric effects by allowing the TACN functionality to be farther from the enzyme active site. Once synthesized, an NPA assay was performed on compound **37** (**Figure 18A**) with bCA and probe concentrations of 2 µM and NPA in excess. The probe decreased bCA activity to 24% which suggests significant binding. A second NPA assay was then performed, addressing different ratios of probe to bCA (**Figure 18B**). During this assay, the bCA concentration was held constant at 2 µM while the probe concentration was changed from 2 µM to 10 µM to 20 µM, which resulted in bCA activities of 80%, 51%, and 38% respectively. These results were not expected, as the 2 µM probe concentration resulted in a much higher percent bCA activity than the first NPA assay had indicated. This lead us to believe that compound **37** was degrading in solution.

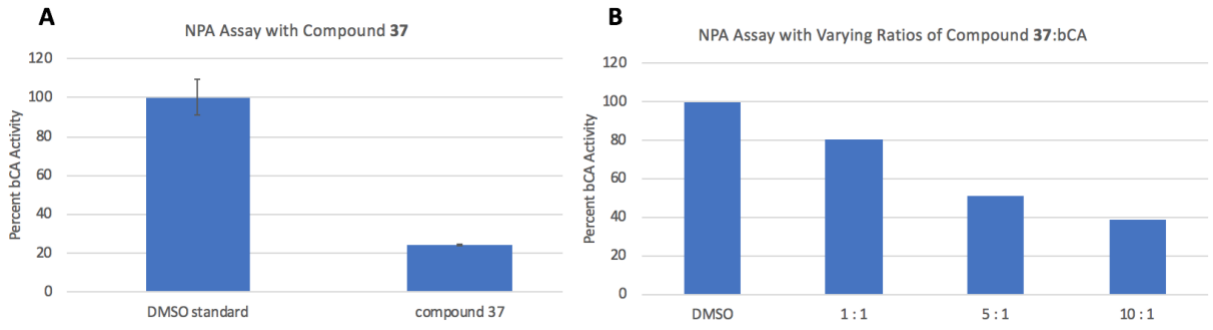

Figure 18: (A) NPA assay with compound **37** in 50mM HEPES buffer with 100 mM KNO_3, pH 7.2, at room temperature. (B) NPA assay comparing different ratios of compound **37** to bCA (1:1, 5:1, and 10:1), performed in 50mM HEPES buffer with 100 mM KNO_3, pH 7.2, at room temperature.

Finally, an NPA assay was performed on compound **38** (**Figure 19**), again with bCA and probe concentrations of 2 µM. The bCA activity was only decreased to 96%, which shows no binding to bCA. Further proof of lack of binding of compounds **37** and **38** to bCA was evident after performing binding studies on a 36 well plate monitoring UV absorbance at 405 nm (**Figure**

20). The probe concentrations were increased from 0 µM to 5 µM. No binding can be observed from these plots and no aggregation was found during a DLS analysis of compound **37**. Based on these results, we think that compounds **37** and **38** degrade quickly in solution. One possible way to remedy this problem would be to store dry aliquots of compounds **37** and **38**, rather than storing them in solution (even storing them at -20 °C did not prevent this fast degradation in solution). It is also speculated that hydrophobic effects are negatively affecting the binding of these probes to CA. Since the fluorine moiety is hydrophobic, the molecules in solution may be arranging themselves in such a way that the hydrophobic (fluorine) side of the molecules are surrounded by the hydrophilic PEG chains. This bulky arrangement would then make it difficult for the sulfonamide groups to enter the CA active site. These results require further investigation.

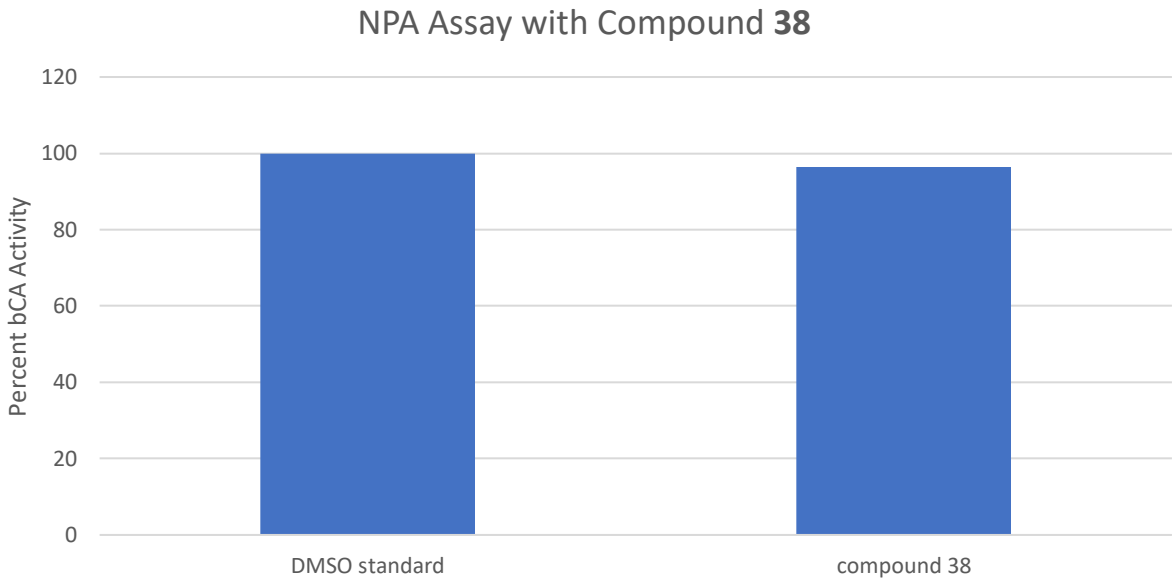

Figure 19: NPA assay with compound **38** performed in 50mM HEPES buffer with 100 mM KNO_3, pH 7.2, at room temperature.

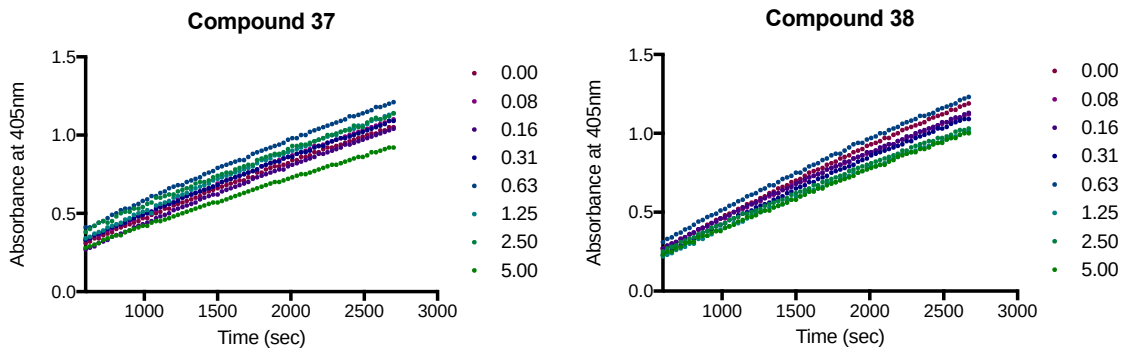

Figure 20: Binding studies monitoring the binding of compounds **37** and **38** with bCA over 2700 seconds, increasing the probe concentrations from 0 µM to 5 µM. This was performed on a 36 well plate measuring absorbance at 405 nm at room temperature.

III. MATERIALS AND METHODS

General

All solvents and chemicals were purchased from Sigma-Aldrich, Acros and Fisher Sci. and used as received. High pressure liquid chromatography (HPLC) was carried out on a Biotage Isolera One. The ^{1}H and ^{19}F NMR spectroscopic measurements were conducted using a 400 MHz AGILENT NMR spectrometer. NMR samples were prepared in CD_3CN, $CDCl_3$, D_2O, or CD_3OD and chemical shifts are reported in ppm. Electrospray Ionization Mass Spectrometry (ESI-MS) was performed on an Agilent 6130 Mass Spectrometer equipped with a UV-Vis detector. Spectroscopic studies were performed using an Agilent Cary 60 UV-Vis Spectrophotometer and an Agilent Cary Eclipse Fluorescence Spectrophotometer. Peptide synthesis was performed using a CEM Liberty Blue Automated Microwave Peptide Synthesizer.

Synthesis

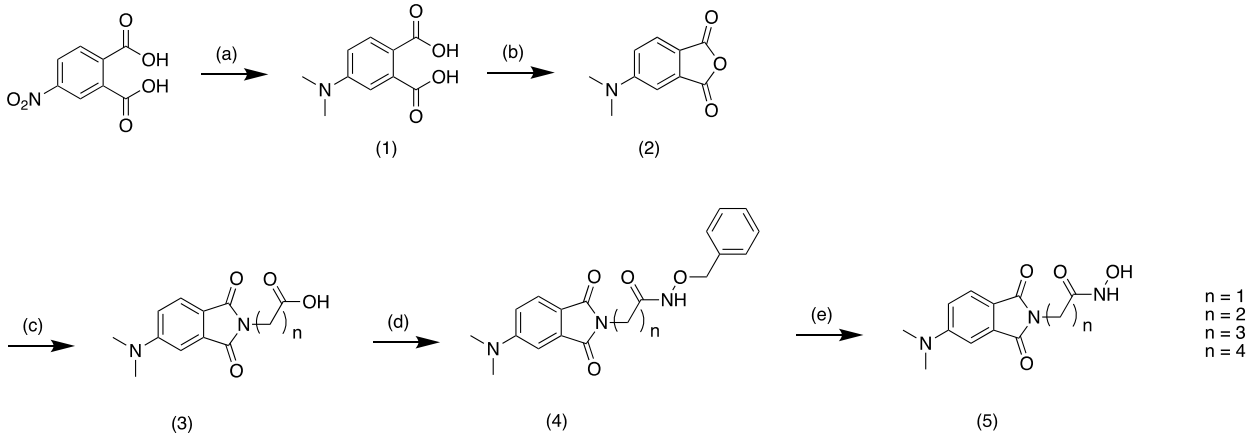

Compound **1**: 4-nitrophthalic acid (420 mg, 2 mmol) was dissolved in methanol (120 mL). Formaldehyde (12 mL, 436 mmol) and palladium on carbon (160 mg, 1.5 mmol) were added to the flask. Finally, hydrogen gas was introduced to the system and the mixture was stirred overnight at RT. The reaction mixture was filtered through a celite pad and washed with methanol (2 x 20 mL). The methanol was concentrated *in vacuo* and this resulted in a yellow solid (0.2319 g, 56%

yield). ^{1}H NMR (400 MHz, Methanol-d4) δ 7.83 (s, 1H), 6.85 (s, 1H), 6.74 (s, 1H), 3.35 (s, 3H), 3.03 (s, 5H).

Compound **2**: Compound **1** (1.4445 g, 6.9 mmol) was put into a sublimation apparatus and heated at 120 °C overnight. Product was a bright yellow solid (0.1857 g, quantitative yield). 1H NMR (400 MHz, Methanol-d4) δ 7.77 (s, 1H), 7.16 (s, 1H), 7.13 (d, J = 8.7 Hz, 1H), 3.17 (s, 6H).

Compound **3.1**: Compound **2** (70 mg, 0.36 mmol) was combined with glycine (27 mg, 0.36 mmol) in toluene (4 mL). Triethylamine (0.1 mL, 0.72 mmol) was added and the solution was refluxed overnight at 115 °C. The product was allowed to cool to RT, the solvent was evaporated, and the crude mixture was taken up in DI water (50 mL). The crude product was extracted with ethyl acetate (3 x 15 mL). The organic layers were washed with brine (1 x 45 mL), dried over sodium sulfate, and concentrated *in vacuo*. Silica column chromatography (gradient, 97:3 DCM:MeOH) gave a yellow solid (35.1 mg, 37% yield).

Compound **3.2**: Compound **2** (70 mg, 0.36 mmol) was combined with beta-alanine (32.608 mg, 0.36 mmol) in toluene (4 mL). Triethylamine (0.1 mL, 0.72 mmol) was added and the solution was refluxed overnight at 115 °C. The product was allowed to cool to RT, the solvent was evaporated, and the crude mixture was taken up in DI water (50 mL). The crude product was extracted with ethyl acetate (3 x 15 mL). The organic layers were washed with brine (1 x 45 mL), dried over sodium sulfate, and concentrated *in vacuo*. Product was purified through PLC (gradient, 99:1 DCM:MeOH) and resulted in a yellow solid (81.6 mg, 85% yield).

Compound **3.3**: Compound **2** (70 mg, 0.36 mmol) was combined with gamma-aminobutyric acid (37.7 mg, 0.36 mmol) in toluene (4 mL). Triethylamine (0.1 mL, 0.72 mmol) was added and the solution was refluxed overnight at 115 °C. The product was allowed to cool to RT, the solvent was evaporated, and the crude mixture was taken up in DI water (50 mL). The crude product was extracted with ethyl acetate (3 x 15 mL). The organic layers were washed with brine (1 x 45 mL), dried over sodium sulfate, and concentrated *in vacuo*. Product was purified through PLC (gradient, 99:1 DCM:MeOH) and resulted in a yellow solid (75 mg, 74% yield).

Compound **3.4**: Compound **2** (70 mg, 0.36 mmol) was combined with 5-aminovaleric acid (43 mg, 0.36 mmol) in toluene (4 mL). Triethylamine (0.1 mL, 0.72 mmol) was added and the solution was refluxed overnight at 115 °C. The product was allowed to cool to RT, the solvent was evaporated, and the crude mixture was taken up in DI water (50 mL). The crude product was extracted with ethyl acetate (3 x 15 mL). The organic layers were washed with brine (1 x 45 mL), dried over sodium sulfate, and concentrated *in vacuo*. Silica column chromatography (gradient, 97:3 DCM:MeOH) gave a yellow solid (78.5 mg, 74% yield).

Compound **4**: Compound **3** (78.5 mg, 0.27 mmol) was taken up in dry chloroform, under nitrogen. O-benzylhydroxylamine (86.2 mg, 0.54 mmol), EDC (77.6 mg, 0.405 mmol), and DIPEA (0.19 mL, 1.08 mmol) were added to the flask and the reaction mixture stirred overnight at room temperature under nitrogen. The crude product was washed with DI water (2 x 20 mL) and the aqueous layers were washed with chloroform (2 x 20 mL). The combined organic layers were washed with brine (1 x 50 mL), dried over sodium sulfate, and concentrated *in vacuo*. Silica column chromatography (gradient, 1:9 MeOH:DCM) resulted in a yellow oil (83.8 mg, 78% yield).

Compound **5**: Compound **4** (83.8 mg, 0.212 mmol) was dissolved in MeOH (10 mL). Four nitrogen/vacuum cycles were performed on the flask. Pd/C (50.5 mg, 0.475 mmol) was added to the solution and four additional nitrogen/vacuum cycles were performed. Finally, H_2 gas was introduced to the flask via balloon. The reaction mixture was stirred overnight at room temperature. The mixture was then filtered through a celite pad, washed with MeOH (3 x 50 mL), and concentrated *in vacuo*. Silica column chromatography (gradient, 75:25 EtOAc:hexanes followed by 5:95 MeOH:DCM) resulted in a yellow oil (6.4 mg, 10% yield). 1H NMR (400 MHz, Chloroform-d) δ 7.63 (d, J = 8.5 Hz, 1H), 7.26 (s, 1H), 7.06 (s, 1H), 6.78 (d, J = 10.9 Hz, 1H), 3.65 (s, 3H), 3.11 (s, 6H), 2.42 (s, 1H), 2.36 (s, 1H), 1.83 (s, 1H), 1.66 (d, J = 24.7 Hz, 5H), 1.25 (s, 1H).

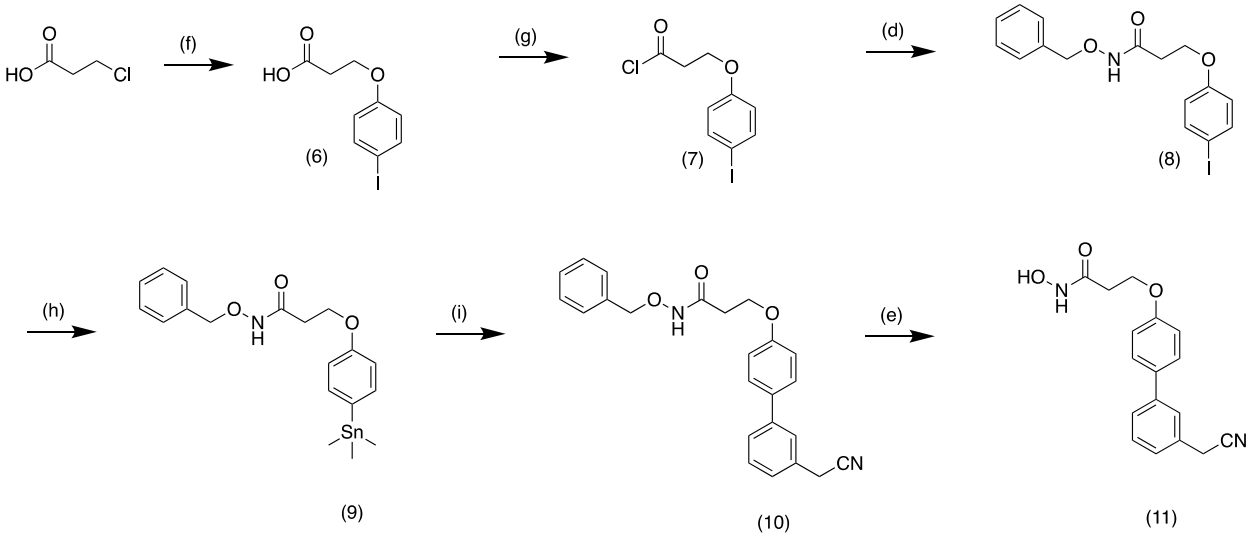

Compound **6**: 3-chloropropionic acid (246 mg, 2.27 mmol) was combined with 4-iodophenol (500 mg, 2.27 mmol). 4.8 M NaOH (1.14 mL) was added dropwise and the reaction stirred at 40 °C overnight. The crude product was taken up in DI water (10 mL) and extracted with EtOAc (3 x 10

mL). The aqueous layer was acidified with concentrated HCl and again the product was extracted with EtOAc (1 x 10 mL). The combined organic layers were dried over $MgSO_4$ and concentrated *in vacuo* which resulted in a beige powder (0.1128 g, 17% yield). 1H NMR (400 MHz, Acetonitrile-d3) δ 7.68 – 7.57 (m, 4H), 6.81 – 6.72 (m, 4H), 6.36 (s, 7H), 4.31 (dtd, J = 7.5, 6.1, 1.4 Hz, 3H), 4.20 (t, J = 6.1 Hz, 4H), 3.83 – 3.73 (m, 2H), 2.83 – 2.71 (m, 6H), 2.70 – 2.58 (m, 3H), 2.49 (td, J = 6.0, 1.1 Hz, 0H), 2.03 – 1.93 (m, 1H), 1.29 (s, 1H).

Compound **7**: Compound **6** (0.1045 g, 0.358 mmol) was dissolved in thionyl chloride (0.624 mL, 8.59 mmol). The solution was heated to reflux (at 80 °C) for thirty minutes. The reaction was then cooled to RT, diluted with diethyl ether (5 mL), and concentrated *in vacuo*. The resulting residue was azeotroped with diethyl ether (3 x 10 mL) and concentrated *in vacuo*, forming a brown oil. The crude product was carried onto the next step.

Compound **8**: Compound **7** (0.11 g, 0.358 mmol) was dissolved in dry chloroform (12 mL) under nitrogen. O-benzylhydroxylamine (0.114 g, 0.716 mmol), EDC (0.103 g, 0.537 mmol), and DIPEA (0.25 mL, 1.432 mmol) were added and the reaction stirred overnight at RT. The reaction mixture was washed with DI water (2 x 12 mL). Remaining product was extracted from the combined aqueous layers with chloroform (2 x 24 mL). The combined organic layers were washed with brine (1 x 20 mL), dried with $MgSO_4$, and concentrated *in vacuo* over silica gel. Flash chromatography (1:99 MeOH:DCM to 15:85 MeOH:DCM) gave a yellow solid (29.5 mg, 21% yield). 1H NMR (400 MHz, Chloroform-d) δ 8.30 (s, 1H), 7.55 (s, 2H), 7.38 (s, 5H), 6.78 – 6.49 (m, 2H), 4.93 (s, 2H), 4.30 – 4.09 (m, 2H), 2.54 (s, 2H).

Compound **9**: Compound **8** (30 mg, 0.076 mmol) was dissolved in dry toluene (2 mL) under nitrogen. Hexamethyldistannane (0.02 mL, 0.0855 mmol) was added to the reaction, followed by $Pd(PPH_3)_4$ (4.4 mg, 0.0038 mmol). The reaction was stirred at RT for ten minutes then heated to reflux (115 °C) for 40 minutes. The reaction mixture was cooled to RT, diluted with EtOAc (10 mL), and filtered. The filtrate was washed with 1 mM PBS buffer at pH 7 (1 x 10 mL) and brine (1 x 10 mL), dried with Na_2SO_4, and concentrated *in vacuo* which resulted in a brown oil (2.21 mg, 66% yield). 1H NMR (400 MHz, Chloroform-d) δ 8.50 (s, 1H), 7.71 – 7.41 (m, 5H), 6.85 (t, J = 17.8 Hz, 3H), 4.92 (s, 3H), 4.20 (s, 4H), 2.56 (s, 2H), 0.27 (s, 9H).

Compound **10**: Compound **9** (0.0212 g, 0.05 mmol) was dissolved in dry toluene (1 mL) under nitrogen. 3-iodophenylacetonitrile (0.0123 g, 0.05 mmol) and $Pd(PPH_3)_4$ (0.0035 g, 0.003 mmol) were added to the mixture and the reaction stirred for ten minutes at RT. The reaction was then heated to reflux (115 °C) for 24 hours, cooled back down to RT, and diluted with EtOAc (20 mL). The product was washed with 1 mM PBS buffer at pH 7 (1 x 20 mL) and brine (1 x 20 mL). The organic layer was dried with Na_2SO_4 and concentrated *in vacuo* which resulted in a yellow product (13.4 mg, 71% yield). 1H NMR (400 MHz, Chloroform-d) δ 7.77 – 7.59 (m, 2H), 7.62 – 7.52 (m, 1H), 7.56 – 7.43 (m, 3H), 7.48 – 7.37 (m, 1H), 7.40 – 7.23 (m, 1H), 6.99 (dd, J = 8.9, 2.8 Hz, 1H), 5.96 (s, 1H), 5.57 (s, 1H), 4.94 (s, 0H), 4.39 – 4.18 (m, 1H), 3.86 – 3.71 (m, 5H), 3.75 – 3.62 (m, 1H), 2.78 – 2.67 (m, 1H), 2.06 (s, 0H), 1.92 – 1.78 (m, 4H), 1.31 – 1.23 (m, 2H), 0.92 – 0.82 (m, 0H), 0.07 (s, 1H).

Compound **11**: Compound **10** (10.8 mg, 0.028 mmol) was dissolved in dry MeOH (1.2 mL). Four nitrogen/vacuum cycles were performed on the flask. Pd/C (6.67 mg, 0.063 mmol) was added to

the solution and four additional nitrogen/vacuum cycles were performed. Finally, H_2 gas was introduced to the flask via balloon. The reaction mixture was stirred overnight at room temperature. The mixture was then filtered through a celite pad, washed with MeOH (3 x 50 mL), and concentrated *in vacuo*. Flash chromatography (75:25 EtOAc:hexanes) gave a yellow product (3.3 mg, 40% yield). 1H NMR (400 MHz, Chloroform-d) δ 8.30 (s, 1H), 7.57 – 7.31 (m, 9H), 4.95 (s, 2H), 4.26 (s, 2H), 2.60 (s, 2H).

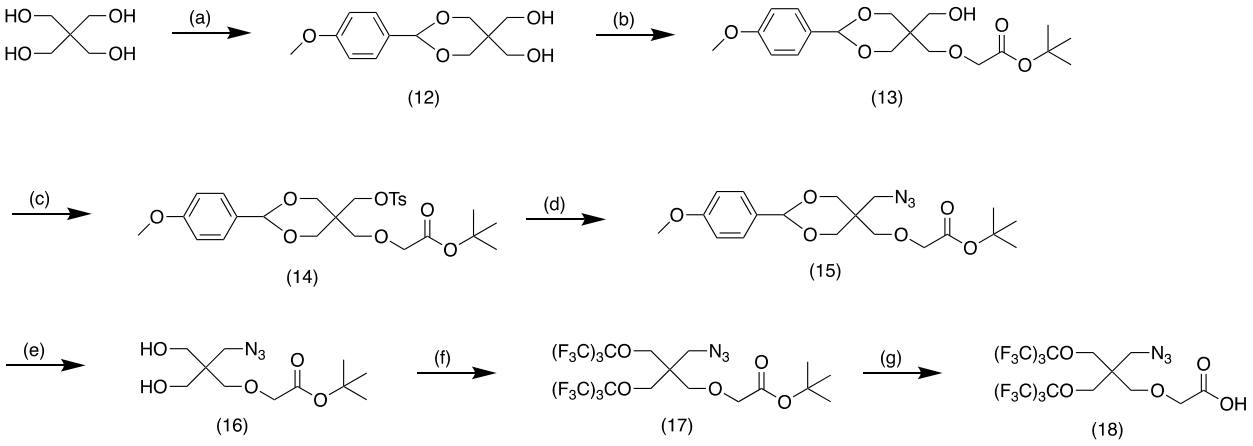

Compound **12**: Pentaerythritol (25 g, 183.6 mmol) was dissolved in DI water (180 mL). The solution was heated to 70 °C. The solution was cooled to RT and concentrated HCl (1 mL) was added to the solution. P-anisaldehyde (1 mL, 8.22 mmol) was added to the solution and the reaction stirred until precipitation. The remaining P-anisaldehyde (22.5 mL, 184.9 mmol) was added to the mixture dropwise via addition funnel and the reaction stirred for three hours. The crude mixture was washed with 0.1 M Na_2CO_3 (1 x 500 mL) and ether (1 x 500 mL). Product was concentrated *in vacuo*.

Compound **13**: Compound **12** (10 g, 39.33 mmol) was put into a 3-neck flask containing a stir bar and chilled in a water and ice bath. Once cooled, dry DMF (100 mL) was added to the flask dropwise. Potassium tert-butoxide, 1.7 M (20% wt.%) solution in THF (25 mL, 206.97 mmol) was added dropwise, followed by tert-butyl 2-bromoacetate (7.6 mL, 51.47 mmol). The reaction was removed from the ice bath and refluxed at 65 °C for two days. The reaction was cooled to RT, filtered, and concentrated *in vacuo*. The product was taken up in 200 mL EtOAc and washed with DI water (1 x 200 mL). Remaining product was extracted from the aqueous layer with DCM (2 x 200 mL). The combined organic layers were dried over sodium sulfate and concentrated *in vacuo*. Silica column chromatography (10:1 hexanes:EtOAc to 2:1 hexanes:EtOAc) resulted in an oil (9 g, 62% yield).

Compound **14**: Compound **13** (9 g, 24.43 mmol) was combined with DMAP (4.48 g, 36.64 mmol) and dissolved in DCM (100 mL). The reaction was cooled to 0 °C. TsCl (6.98 g, 36.64 mmol) was added and the reaction warmed up to RT and stirred overnight. The product was washed with $NaHCO_3$ (2 x 50 mL) and brine (3 x 50 mL), dried over sodium sulfate, and concentrated *in vacuo*. Silica column chromatography (10:1 hexanes:EtOAc to 4:1 hexanes:EtOAc) resulted in an oil (8 g, 62% yield).

Compound **15**: Sodium azide (1.5 g, 22.95 mmol) was combined with compound **14** (8 g, 15.3 mmol) and dissolved in DMF (80 mL). Flask was flushed with nitrogen and heated to 120 °C for two days. The mixture was cooled to RT, taken up in Milli-Q water (160 mL), and extracted with DCM (3 x 160 mL). The combined organic layers were washed with brine (1 x 200 mL), dried

over sodium sulfate, and concentrated *in vacuo*. Silica column chromatography (20:3 hexanes:EtOAc) resulted in an oil (3 g, 50% yield).

Compound **16**: Compound **15** (3 g, 7.6 mmol) was dissolved in 4:1 HOAc:H_2O (25 mL) and stirred at 40 °C for three hours. Reaction brought back to RT and concentrated *in vacuo*. Sodium bicarbonate (50 mL) in water (50 mL) was used to neutralize the reaction. The product was extracted with EtOAc (3 x 25 mL), dried over sodium sulfate, and concentrated *in vacuo*. Silica column chromatography (10:1 hexanes:EtOAc to 2:1 hexanes:EtOAc) resulted in an oil (1.96 g, 93% yield).

Compound **17**: PPh_3 (6.36 g, 24.26 mmol) was dissolved in dry THF (35 mL) and cooled to 0 °C. DIAD (4.88 g, 24.26 mmol) was added to the flask along with additional THF (5 mL). The reaction was removed from ice and stirred for 20 minutes. Nitrogen was introduced to the system. Compound **16** (2.2261 g, 8.086 mmol) was dissolved in dry THF (40 mL) and added in small batches to the reaction. C_4HF_9O (3.38 mL, 24.26 mmol) was added to the reaction. The solution was removed from nitrogen and stirred for three days at RT. The solution was concentrated *in vacuo* over silica gel. Silica column chromatography (pure hexanes to 20:1 hexanes:DCM) resulted in an opaque oil product (3.314 g, 58% yield).

Compound **18**: Compound **17** (2 g, 2.8 mmol) was combined with TIS (0.26 mL, 1.27 mmol) and Milli-Q water (0.26 mL, 14.44 mmol). The reaction was cooled to 0 °C and TFA (10 mL, 130.59 mmol) was added. The reaction stirred overnight and was allowed to warm to RT. The solution was concentrated *in vacuo* and azeotroped with DCM (3 x 10 mL). The crude product was

concentrated *in vacuo* over silica gel. Silica column chromatography (pure DCM to 8:1 DCM:MeOH with 0.5% HOAc) resulted in the product (0.9146 g, 50% yield).

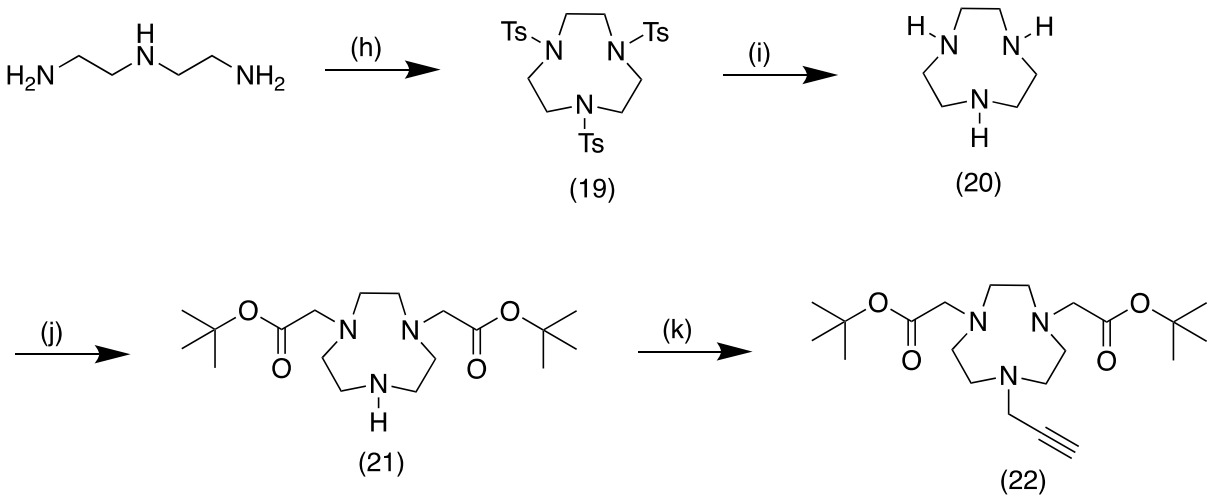

Compound **19**: Synthesized by Dr. Meng Yu.

Compound **20**: Synthesized by Dr. Meng Yu.

Compound **21**: Compound **20** (1.2 g, 9.29 mmol) was added to a flask under nitrogen. Dry chloroform (30 mL) was added to compound **20** and the reaction was placed over an ice bath. Sodium bicarbonate (1.56 g, 18.58 mmol) was added to the solution, followed by tert-butyl bromoacetate (3.17 mL, 21.47 mmol) dropwise. More chloroform (50 mL) was added and the reaction stirred under nitrogen overnight at RT. The crude product was concentrated *in vacuo* over celite. Flash chromatography (pure water with formic acid to 30:70 ACN:water) resulted in the pure product.

Compound **22**: Compound **21** (10 mg, 0.028 mmol) was dissolved in dry acetonitrile (5 mL). Potassium carbonate (9.665 mg, 0.07 mmol) was added and the reaction stirred for 20 minutes. The reaction was placed over an ice bath and 3-bromoprop-1-yne (0.028 mL, 0.3424 mmol) was added dropwise (under nitrogen). The ice bath was removed and the reaction stirred at RT for two days. LCMS confirmed product formation.

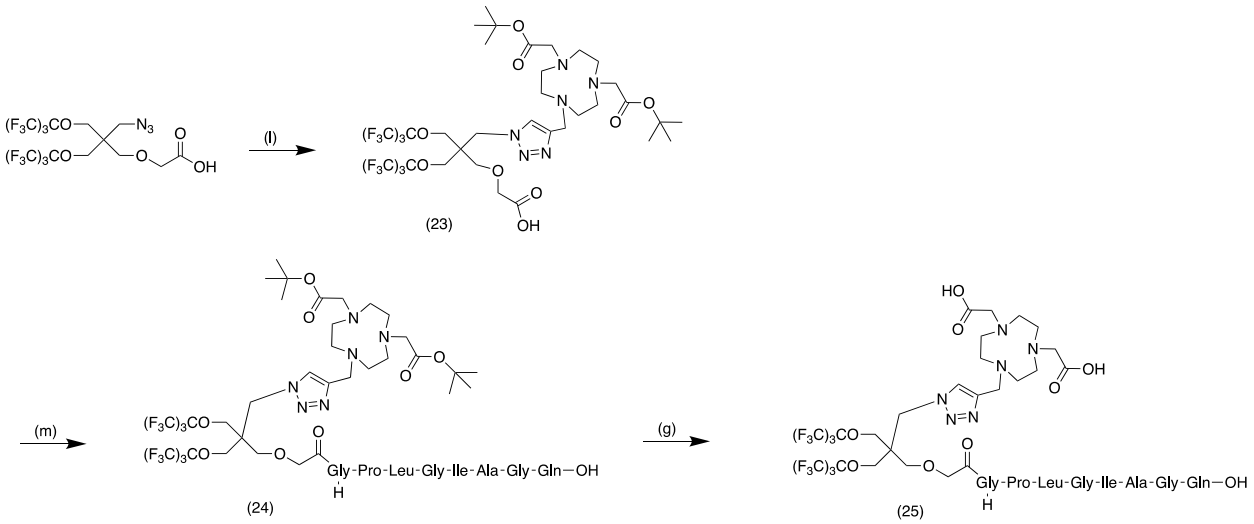

Compound **23**: Compound **22** (0.247 g, 0.6245 mmol) was combined with compound **18** (0.341 g, 0.5204 mmol) in dry DCM (5 mL). Ascorbic acid (0.0206 g, 0.1041 mmol) and copper sulfate (6.5 mg, 0.02602 mmol) were combined and dissolved in degassed water (5 mL). The water solution was added to the DCM solution and stirred in a glove box overnight at RT. Added 0.05 equivalents more of copper sulfate and 0.2 equivalents more of ascorbic acid; reaction stirred another night. The solution was washed with chloroform (3 x 20 mL). The combined organic layers were dried over sodium sulfate and concentrated *in vacuo* over celite. Flash chromatography resulted in pure product (340 mg, 62% yield).

Compound **24**: Peptide (Gly-Pro-Leu-Gly-Ile-Ala-Gly-Gln) (0.117 g, 0.035 mmol) was added to a filtered syringe. Dry DCM (4 mL) was added and the resin was allowed to swell for ten minutes. The DCM was ejected. Compound **23** (55.17 mg, 0.0525 mmol), DIPEA (0.04877 mL, 0.280 mmol), and HATU (26.62 mg, 0.07 mmol) were combined in DMF (5 mL) and stirred for ten minutes under nitrogen. The DMF solution was pulled up into the filtered syringe containing the peptide and the reaction mixed on a shaker overnight. The solution was ejected and washed with DMF (3 x 5 mL), DCM (3 x 5 mL), and MeOH (3 x 5 mL). Product dried on lyophilizer. Product was confirmed through LCMS.

Compound **25**: Compound **24** (0.117 g, 0.0867 mmol) was combined with TFA (5 mL, 65.3 mmol), TIS (0.26 mL, 1.27 mmol) and Milli-Q water (0.26 mL, 14.44 mmol) in a filtered syringe. The reaction was mixed on a shaker for three hours. The solution was concentrated *in vacuo*. Flash chromatography (45:55 ACN:water) resulted in a solid (8 mg, 9% yield). 19F NMR (376 MHz, Deuterium Oxide) δ -70.68.

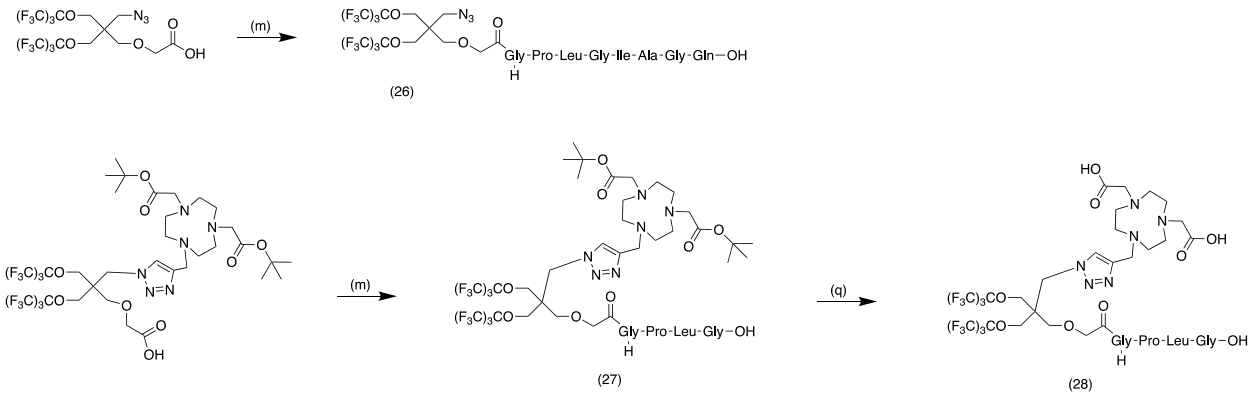

Compound **26**: Peptide (Gly-Pro-Leu-Gly-Ile-Ala-Gly-Gln) (0.140 g, 0.049 mmol) was added to a filtered syringe. Dry DCM (4 mL) was added and the resin was allowed to swell for ten minutes.

The DCM was ejected. Compound **18** (64.21 mg, 0.098 mmol), DIPEA (0.03414 mL, 0.196 mmol), and HATU (37.26 mg, 0.098 mmol) were combined in DMF (3 mL) and stirred for ten minutes under nitrogen. The DMF solution was pulled up into the filtered syringe containing the peptide and the reaction mixed on a shaker overnight. The solution was ejected and washed with DMF (3 x 5 mL), DCM (3 x 5 mL), and MeOH (3 x 5 mL). Product dried on lyophilizer. The crude product was combined with TFA (5 mL, 65.3 mmol), TIS (0.26 mL, 1.27 mmol) and Milli-Q water (0.26 mL, 14.44 mmol) in a filtered syringe. The reaction was mixed on a shaker for three hours. The solution was concentrated *in vacuo*. Flash chromatography (0:100 to 40:60 to 100:0 ACN:water) resulted in a solid (13 mg, 9% yield). 19F NMR (376 MHz, Deuterium Oxide) δ -70.53.

Compound **27**: Peptide (Gly-Pro-Leu-Gly) (0.117 g, 0.0351 mmol) was added to a filtered syringe. Dry DCM (4 mL) was added and the resin was allowed to swell for ten minutes. The DCM was ejected. Compound **23** (44.3 mg, 0.04212 mmol), 2,4,6-collidine (0.01827 mL, 0.1404 mmol), and PyAOP (36.6 mg, 0.0702 mmol) were combined in DMF (3 mL) and stirred for ten minutes under nitrogen. The DMF solution was pulled up into the filtered syringe containing the peptide and the reaction mixed on a shaker overnight. The solution was ejected and washed with DMF (3 x 5 mL), DCM (3 x 5 mL), and MeOH (3 x 5 mL). Product dried through lyophilization and taken onto the next step.

Compound **28**: Compound **27** was combined with TFA (5 mL, 65.3 mmol), TIS (0.26 mL, 1.27 mmol) and Milli-Q water (0.26 mL, 14.44 mmol) in a filtered syringe. The reaction was mixed on a shaker for three hours. The solution was concentrated *in vacuo*. Flash chromatography (0:100 to

40:60 to 100:0 ACN:water) resulted in a solid (14.3 mg, 27% yield). 19F NMR (376 MHz, Deuterium Oxide) δ -71.41 (d, J = 29.3 Hz).

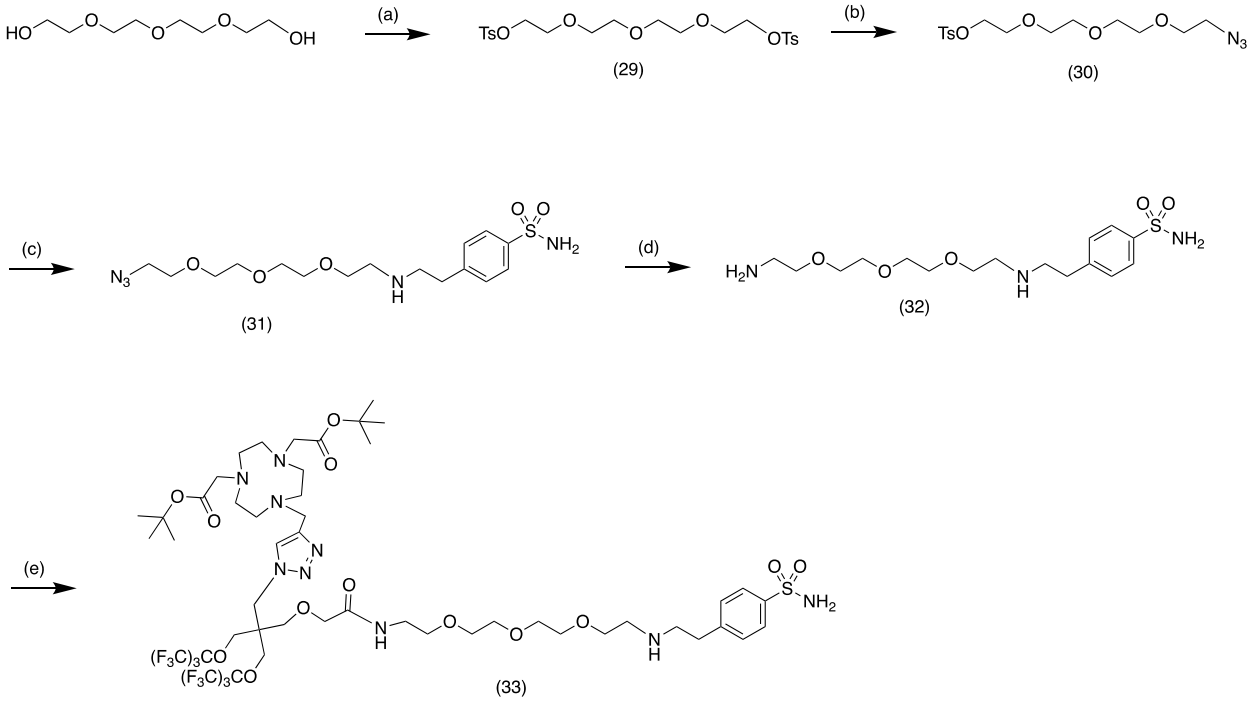

Compound **29**: Tetraethylene glycol (3 g, 15.45 mmol) was dissolved in dry DCM (40 mL). TEA (4.31 mL, 30.89 mmol) was added and the solution was cooled to 0 °C. P-toluenesulfonylchloride (8.84 g, 46.35 mmol) was added portion-wise to the reaction. The solution was allowed to warm to RT and stirred overnight under nitrogen. The solution was washed with saturated sodium bicarbonate (3 x 40 mL) and dried over sodium sulfate. The organic layers were concentrated *in vacuo*. Silica column chromatography (50:50 hexanes:DCM) resulted in an oil (6.1027 g, 79% yield).

Compound **30**: Compound **29** (6.1027 g, 12.14 mmol) was dissolved in ethanol (50 mL) and cooled to 0 °C, under nitrogen. Sodium azide (0.789 g, 12.14 mmol) was measured out with a plastic spatula and added to the reaction over 20 minutes. The reaction was heated to reflux (80 °C) and stirred overnight, under nitrogen. The reaction was cooled to RT and taken up in DCM (50 mL) and washed with saturated sodium bicarbonate (1 x 100 mL). The organic layer was dried over sodium sulfate and concentrated *in vacuo*. Silica column chromatography (75:25 hexanes:EtOAc) resulted in a yellow oil (1.1871 g, 26% yield).

Compound **31**: Compound **30** (22.3 mg, 0.0599 mmol), 4-(2-aminoethyl)benzenesulfonamide (10 mg, 0.0499 mmol), and potassium carbonate (10.34 mg, 0.075 mmol) were combined in dry DMF (3 mL) under nitrogen. The reaction was heated to 80 °C overnight. The reaction mixture was cooled to RT and concentrated *in vacuo*. The crude product was taken up in DI water (5 mL) and extracted with EtOAc (3 x 5 mL). The organic layers were washed with brine (1 x 5 mL), dried over sodium sulfate, and concentrated *in vacuo*. Silica prep plate chromatography (1:1:1 MeOH:acetone:DCM) resulted in an oil (8.4 mg, 35% yield).

Compound **32**: Compound **31** (8.4 mg, 0.0209 mmol) was diluted with dry MeOH (2 mL). Four vacuum/nitrogen cycles were performed on the reaction flask. Pd/C (5 mg, 0.0469 mmol) was added to the reaction and four additional vacuum/nitrogen cycles were preformed. H_2 gas was introduced to the reaction via balloon and the reaction stirred overnight at RT. The mixture was filtered through a celite pad, rinsed with MeOH (3 x 50 mL), and concentrated *in vacuo*, resulting in product (11 mg, quantitative yield).

Compound **33**: Compound **32** (11 mg, 0.0293 mmol) was combined with compound **23** (33.86 mg, 0.0322 mmol) and HATU (22.43 mg, 0.059 mmol) and the flask was dried under vacuum for 30 minutes. Dry DMF (1 mL) and dry DCM (1 mL) were added to the flask, followed by DIPEA (0.02042 mL, 0.1172 mmol). The reaction stirred overnight at RT under nitrogen. The reaction was concentrated *in vacuo* and then taken up in DI water (5 mL). The product was extracted with DCM (3 x 5 mL) and the combined organic layers were dried over sodium sulfate and concentrated *in vacuo*. Silica prep plate chromatography (5:95 MeOH:DCM) resulted in product (4.3 mg, 10% yield). 1H NMR (400 MHz, Methanol-d4) δ 8.51 (d, J = 23.1 Hz, 2H), 8.46 – 8.32 (m, 1H), 8.26 (d, J = 13.6 Hz, 1H), 7.87 – 7.70 (m, 2H), 7.42 (d, J = 8.0 Hz, 2H), 1.47 (q, J = 4.3, 3.0 Hz, 18H). 19F NMR (376 MHz, Methanol-d4) δ -71.27 – -71.56 (m).

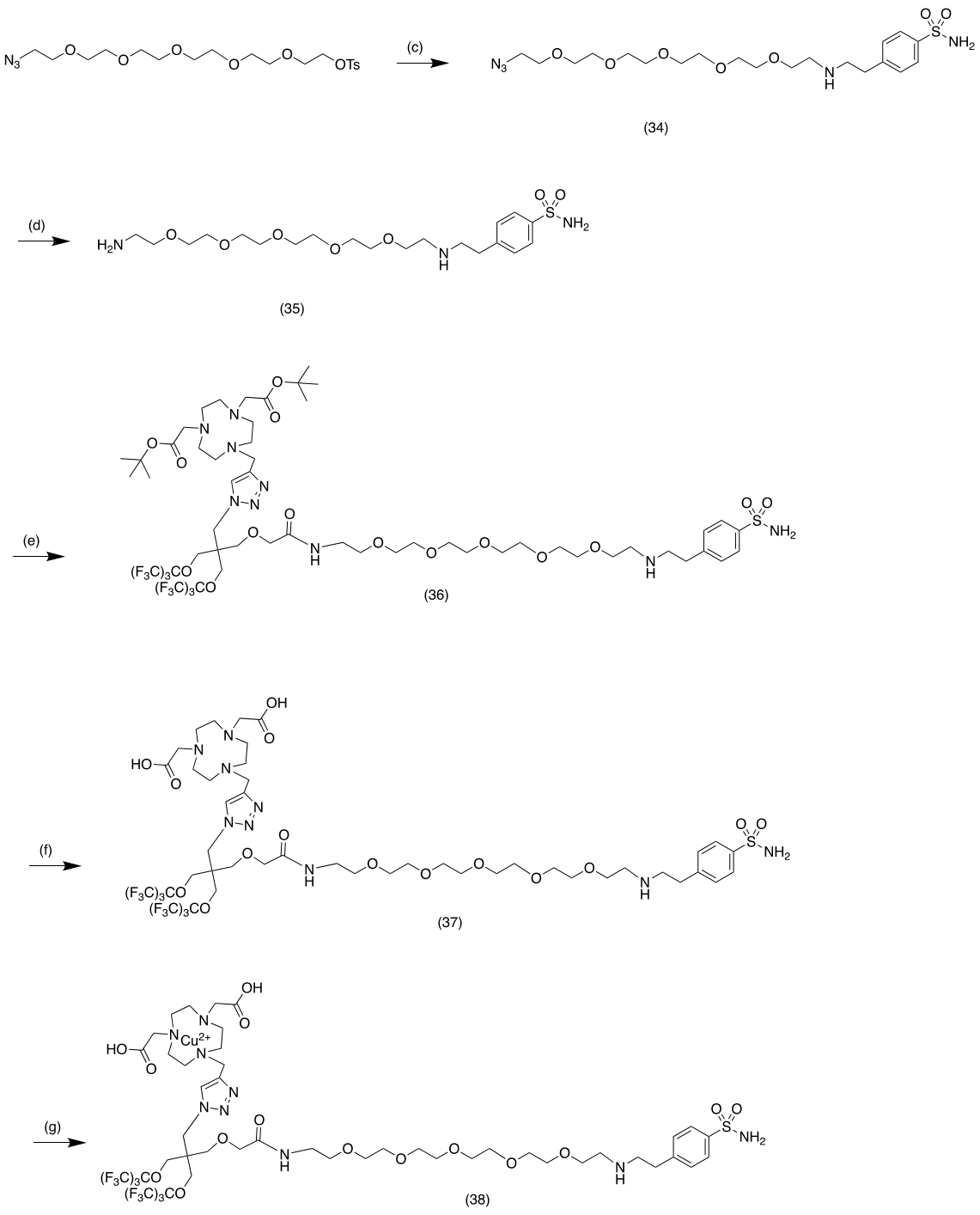

Compound **34**: 17-azido-3,6,9,12,15-pentaoxaheptadecyl 4-methylbenzenesulfonate (27.6 mg, 0.0599 mmol) was added to a flask containing 4-(2-aminoethyl)benzenesulfonamide (10 mg, 0.0499 mmol) and potassium carbonate (10.34 mg, 0.075 mmol) in dry THF (3 mL). The reaction

was heated to 80 °C and stirred overnight under nitrogen. The reaction was cooled to RT and concentrated *in vacuo*. Product was taken up in DI water (5 mL) and extracted with EtOAc (3 x 5 mL). The combined organic layers were washed with brine (1 x 15 mL), dried over sodium sulfate, and concentrated *in vacuo*. Silica prep plate chromatography (1:1:1 MeOH:acetone:DCM) gave pure product (8.4 mg, 29% yield).

Compound **35**: Compound **34** (19 mg, 0.04 mmol) was diluted with dry MeOH (1 mL) and dry DCM (1 mL). Four vacuum/nitrogen cycles were performed on the reaction flask. Pd/C (9.22 mg, 0.09 mmol) was added to the reaction and four additional vacuum/nitrogen cycles were preformed. H_2 gas was introduced to the reaction via balloon and the reaction stirred overnight at RT. The mixture was filtered through a celite pad, rinsed with MeOH (3 x 50 mL), and concentrated *in vacuo*, resulting in product (17 mg, 94% yield).

Compound **36**: Compound **35** (6.9 mg, 0.015 mmol) was combined with compound **23** (17.34 mg, 0.0164 mmol) and PyBOP (15.62 mg, 0.03 mmol) and the flask was dried under vacuum for 30 minutes. Dry DMF (2 mL) was added to the flask, followed by DIPEA (0.01045 mL, 0.06 mmol). The reaction stirred overnight at RT under nitrogen. The reaction was concentrated *in vacuo* and then taken up in DI water (5 mL). The product was extracted with DCM (3 x 5 mL) and the combined organic layers were dried over sodium sulfate and concentrated *in vacuo*. Flash chromatography (76:24 MeOH:water) resulted in pure product (10.7 mg, 48% yield).

Compound **37**: Compound **36** was combined with TIS (0.26 mL, 1.27 mmol) and Milli-Q water (0.26 mL, 14.44 mmol). The reaction was cooled to 0 °C and TFA was added (5 mL, 65.3 mmol).

The reaction was allowed to warm to RT and stirred overnight. The solution was azeotroped with DCM (3 x 5 mL) and concentrated *in vacuo*. Flash chromatography (0:100 to 75:25 to 100:0 MeOH:water) resulted in pure product (13.9 mg, quantitative yield).

Compound **38**: Compound **37** (13.9 mg, 0.01004 mmol) was dissolved in Milli-Q water (1 mL). The pH was adjusted to 7 with 1 M NaOH (1 drop). Copper acetate (2.21 mg, 0.01105 mmol) was added to the solution and the reaction stirred at RT for three hours. Flash chromatography (0:100 to 45:55 to 75:25 to 100:0 NH_4OAc:ACN) resulted in pure product (4.6 mg, 32% yield). 1H NMR (400 MHz, Deuterium Oxide) δ 12.43 (s, 3H), 9.33 – 9.27 (m, 2H), 8.86 (t, J = 7.3 Hz, 2H), 8.55 (d, J = 7.8 Hz, 2H), 8.28 – 8.17 (m, 4H), 4.28 (s, 2H), 3.65 (s, 4H), 3.52 (s, 21H), 3.30 (s, 4H), 2.49 (s, 10H).

Solvent Studies: Stock solutions of the fluorophores were prepared as 10 mM solutions in DMSO. The probe stock solution (0.3 µL, 0.1 µM) was added to 3 mL of the solvent being studied (either chloroform, methanol, DMSO, water, or toluene). The UV-Vis absorbance and fluorescence intensity were measured for each fluorophore, at concentrations of 1 – 10 µM.

bCA Binding Studies: Stock solutions of the fluorophores were prepared as 10 mM solutions in DMSO. The probe stock solution (5 µM) was added to HEPES buffer (pH 7.2, 500 µL) at room temperature. Absorbance and intensity data was collected over a range of concentrations (1 µM – 5 µM). This was performed without any bCA, as a standard. Then, the experiment was performed with bCA; the fluorophore was added first, followed by increasing concentrations of bCA (1 µM

– 5 μM) and then vice versa. Finally, this study was performed with 20 μM, 40 μM, and 60 μM fluorophore compared to 5 μM bCA.

Peptide Synthesis: Peptides were synthesized through solid-phase peptide synthesis (SPPS). All amino acids were F-moc protected and Wang resin was used and supplied in polystyrene beads. Following synthesis, the beads were washed with DMF (3 x 10 mL), DCM (3 x 10 mL), and MeOH (3 x 10 mL) and dried through lyophilization. Separation of the peptides from the beads was accomplished through standard TFA de-protection methods (see above for experimental details).

NPA Assay: Probe stock solutions were prepared as 10 mM DMSO solutions. The CA stock solution was prepared as 350 μM solution in 50 mM HEPES with 100 mM KNO_3, pH 7.2. The NPA stock solution was prepared as 125 mM acetonitrile solution. A typical NPA experiment was carried out by adding HEPES (500 μL), then NPA stock solution (1 μL, 250 μM), probe (0.1 μL, 2.0 μM), and finally CA (2.8 μL, 2.0 μM) to a quartz cuvette. The absorbance was scanned 7 times, the interval between each scan was 90 seconds.

DNSA Assay: Probe stock solutions were prepared as 100 μM DMSO solutions. The CA stock solution was prepared as a 2 mg/mL solution in 50 mM HEPES, 100 mM KNO_3, pH 7.2. The DNSA solution was prepared as 1 mM in DMSO. The excitation setting on the fluorimeter was 280 nm, slit width of 10. The emission was set to 300 – 600 nm, slit width of 10. 1 mL of HEPES was added to a quartz cuvette to collect a baseline. CA (3.5 μL, 0.25 μM) was added to the cuvette. DNSA (2.5 μL, 2.5 μM) was then added. Finally, probe (0.5 μL, 0.05μM) was added and the

emission spectra was measured. Probe was added ten times, for a final concentration of 0.5 μM; an emission spectrum was gathered after each addition.

IV. APPENDIX

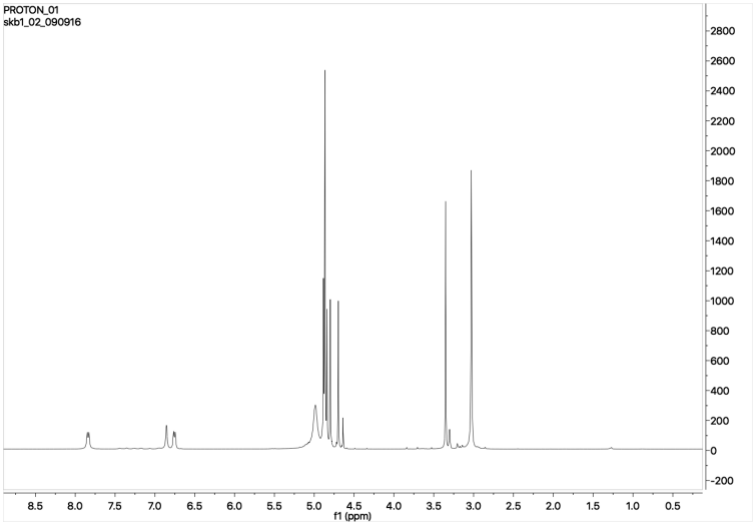

Figure 21: ^{1}H NMR of compound **1**.

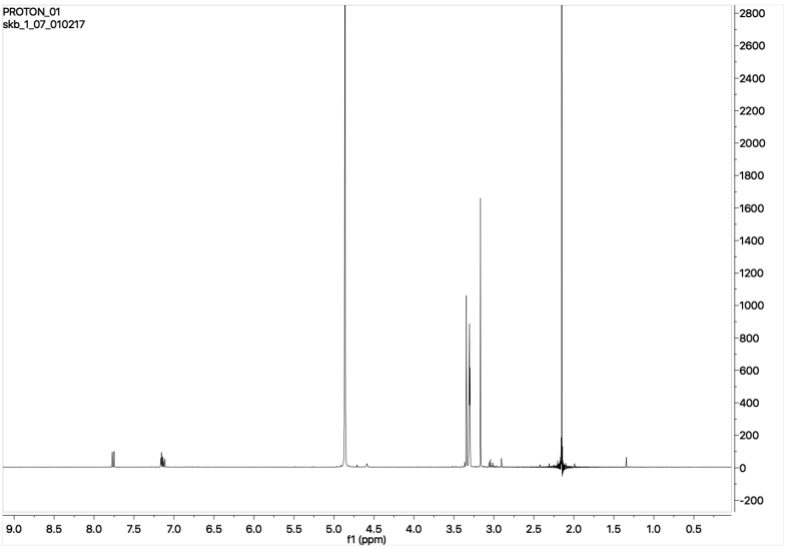

Figure 22: ^{1}H NMR of compound **2**.

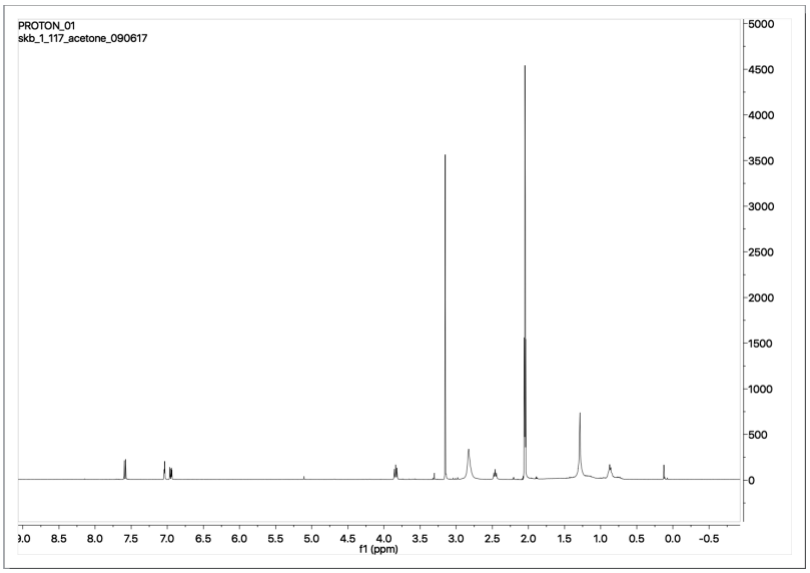

Figure 23: ^{1}H NMR of compound **5.1**.

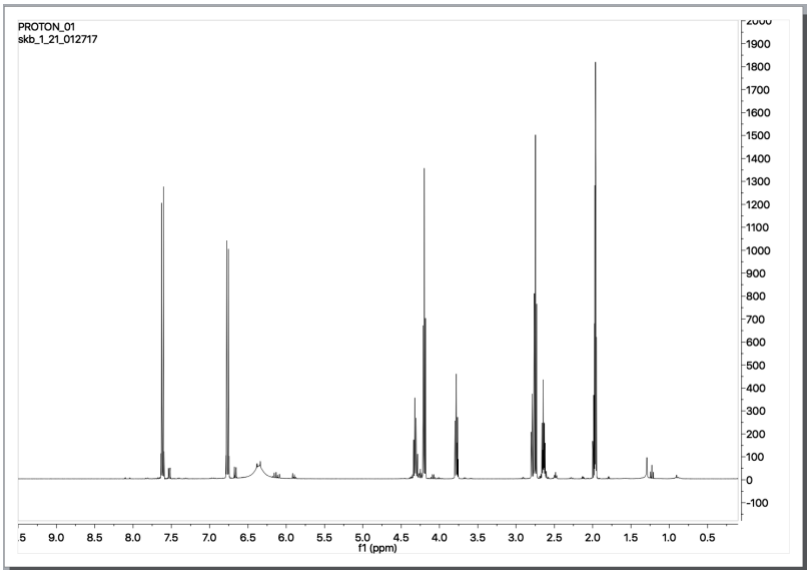

Figure 24: ^{1}H NMR of compound **6**.

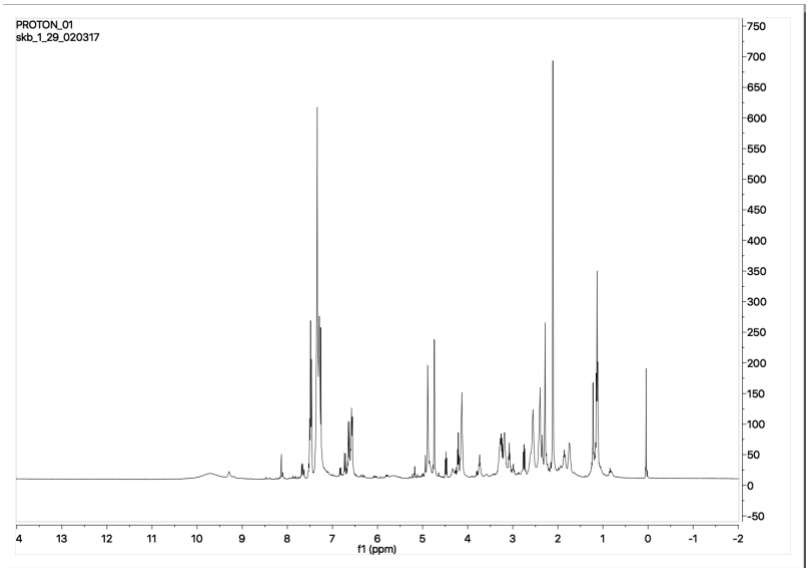

Figure 25: ^{1}H NMR of compound **8**.

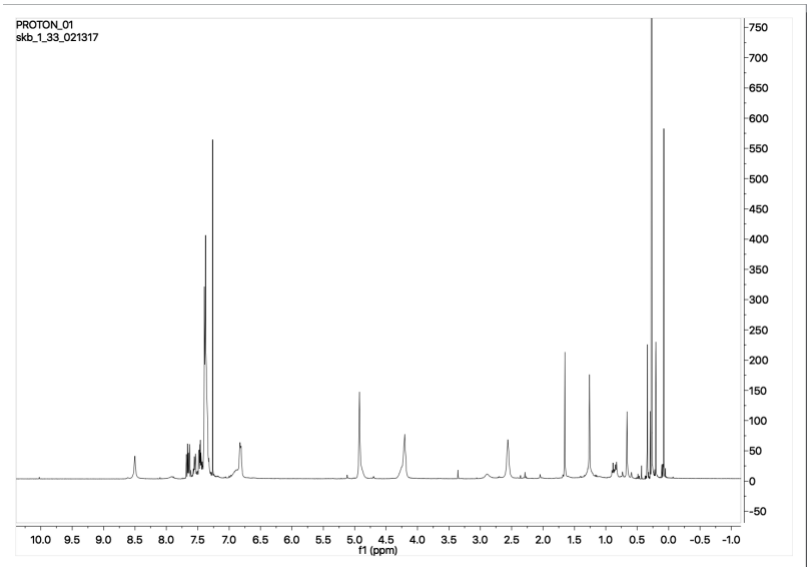

Figure 26: ^{1}H NMR of compound **9**.

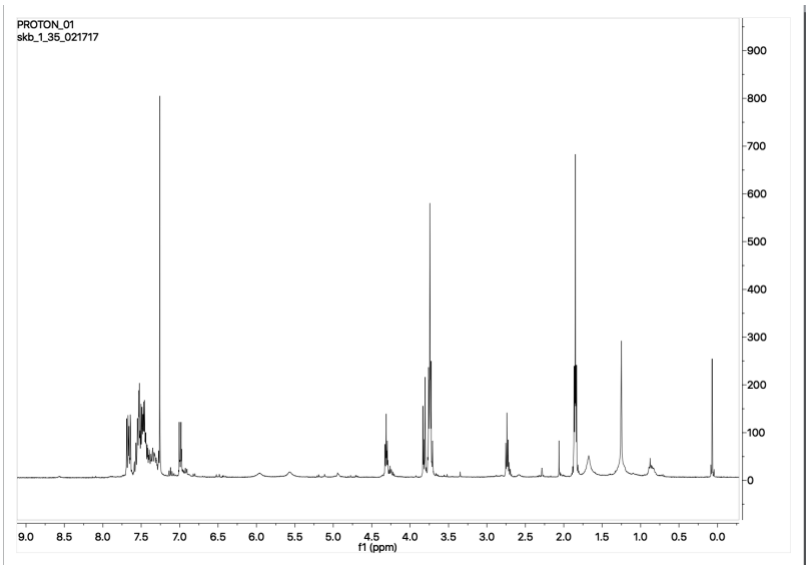

Figure 27: ^{1}H NMR of compound **10**.

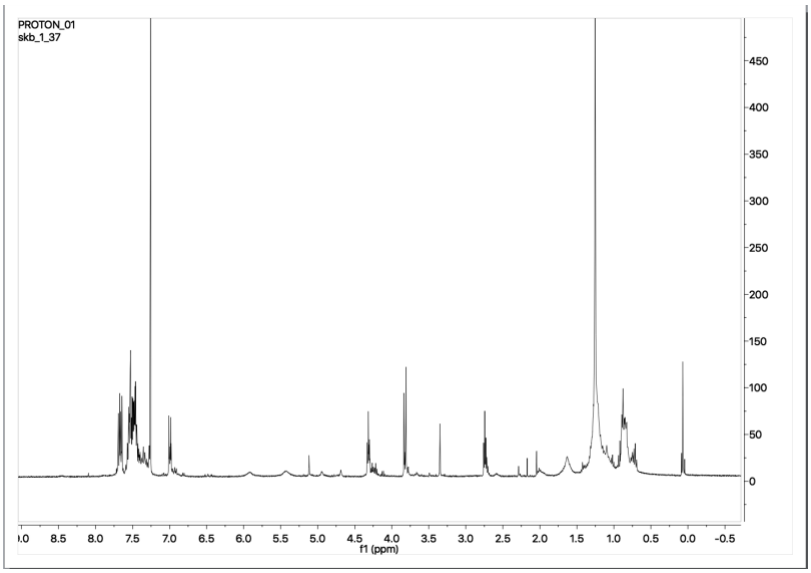

Figure 28: ^{1}H NMR of compound **11**.

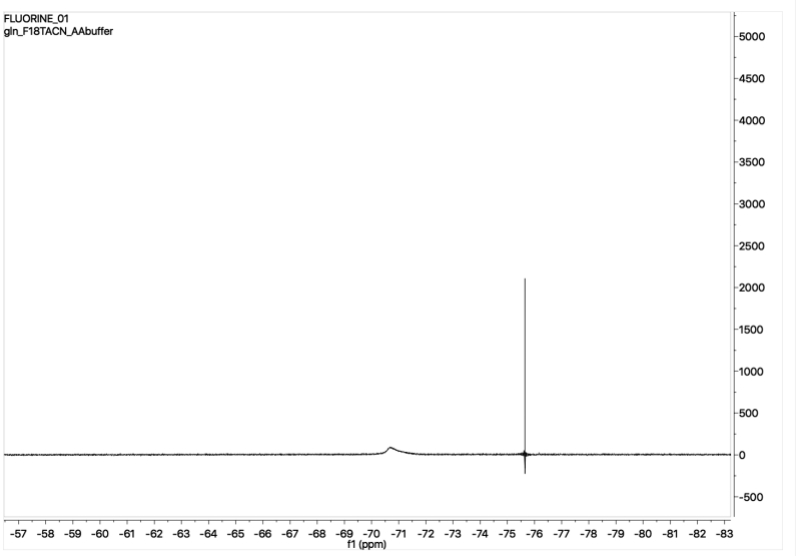

Figure 29: ^{19}F NMR of compound **25**.

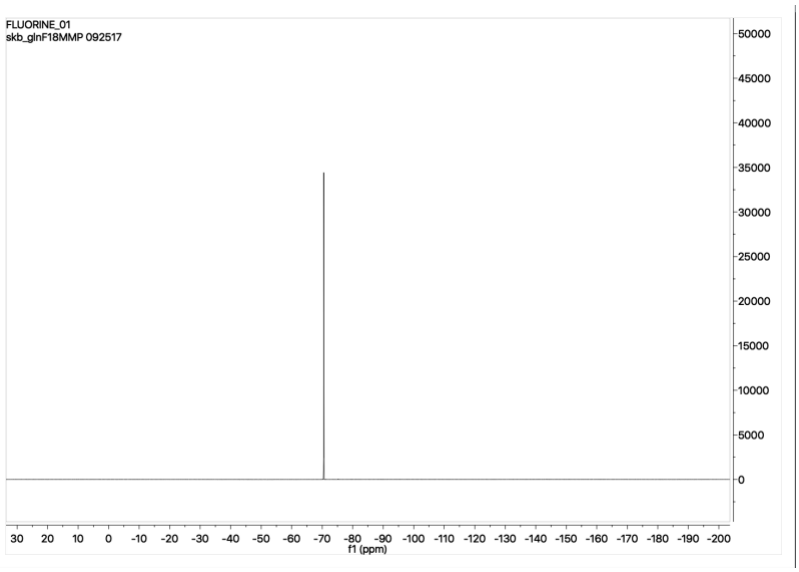

Figure 30: ^{19}F NMR of compound **26**.

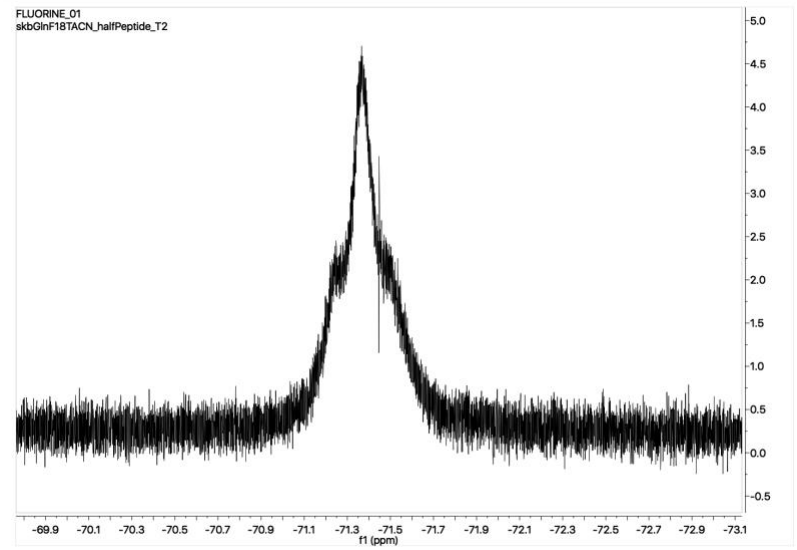

Figure 31: ^{19}F NMR of compound **28**.

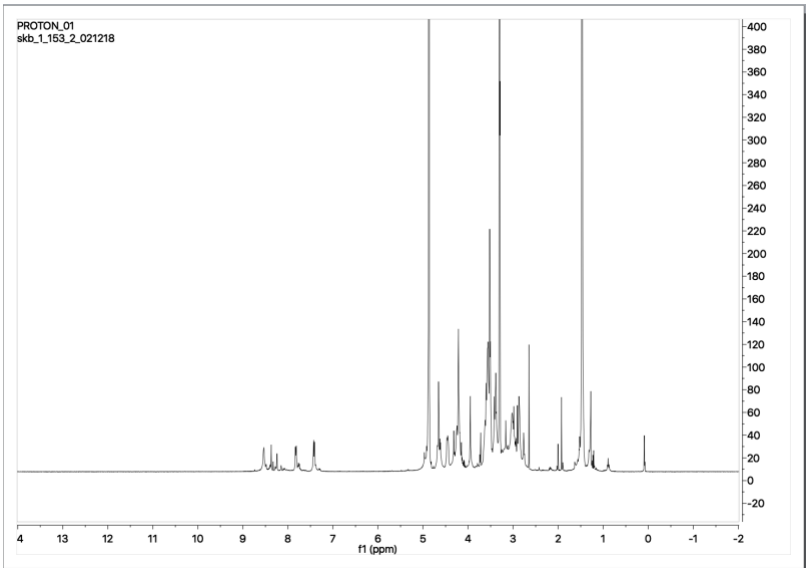

Figure 32: ^{1}H NMR of compound **33**.

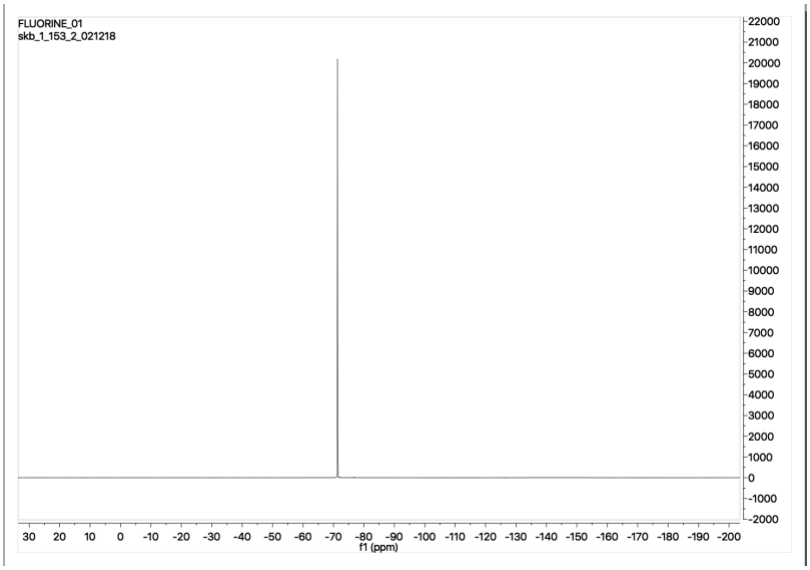

Figure 33: ^{19}F NMR of compound **33**.

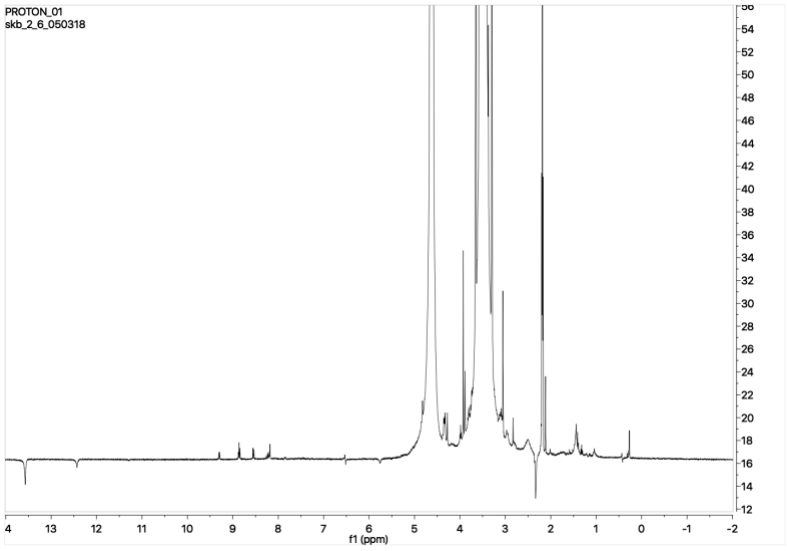

Figure 34: ^{1}H NMR of compound **38**.

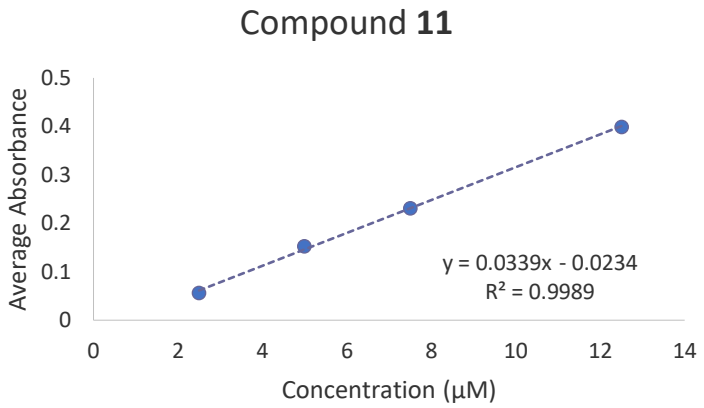

Figure 35: Beer's Law of compound **11**.

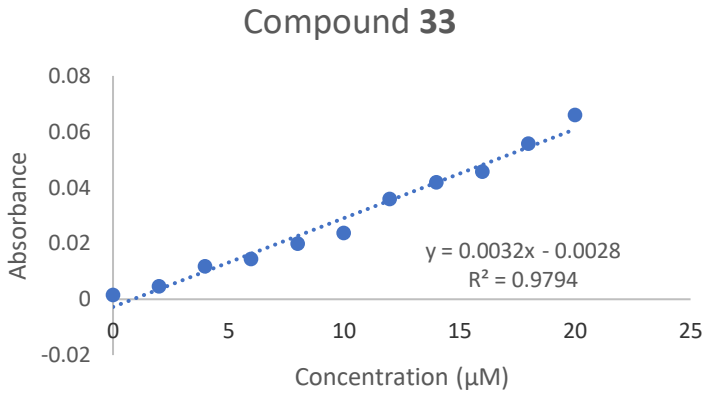

Figure 36: Beer's Law of compound **33** (trial 1).

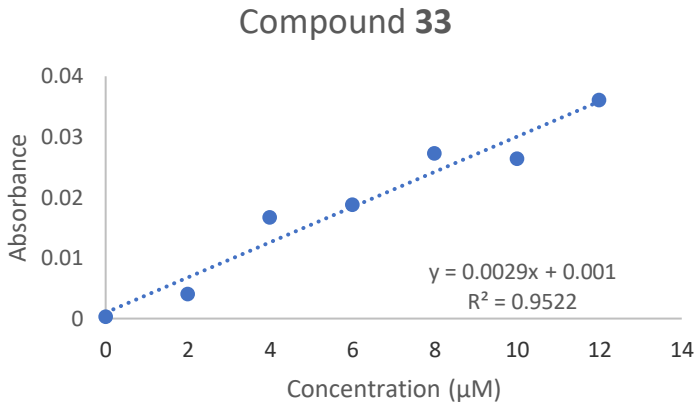

Figure 37: Beer's Law of compound **33** (trial 2).

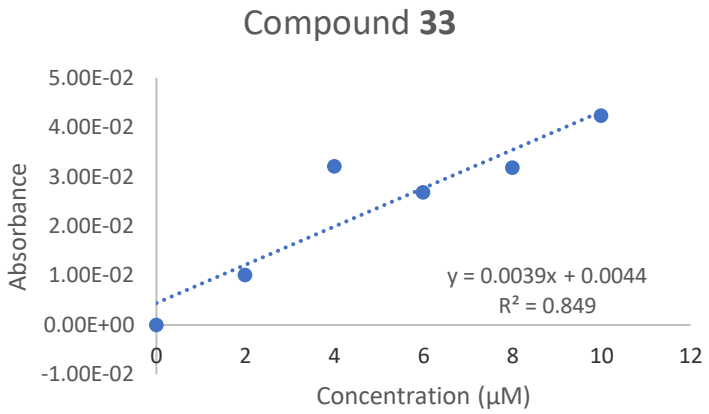

Figure 38: Beer's Law of compound **33** (trial 3).

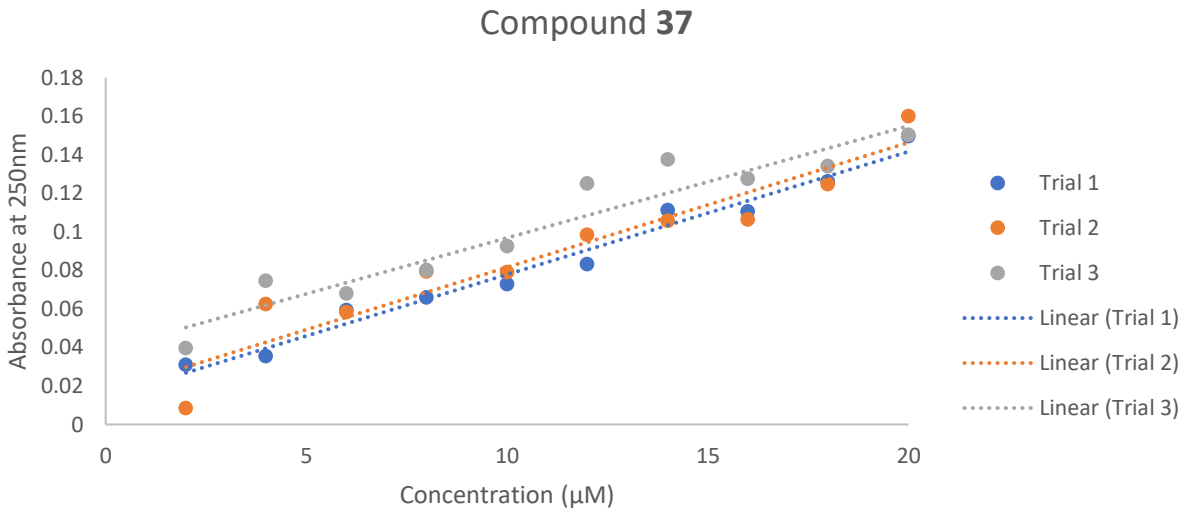

Figure 39: Beer's Law of compound **37**.

V. REFERENCES

1. Anzellotti, A. I.; Farrell , N. P., Zinc metalloproteins as medicinal targets. *Royal Society of Chemistry* **2008,** *37*, 1629-1651.
2. McCall, K. A.; Huang, C.; Fierke, C. A., Function and mechanism of zinc metalloenzymes. *J Nutr* **2000,** *130* (5S Suppl), 1437S-46S.
3. Rundhaug, J. E., Matrix Metalloproteinases, Angiogenesis, and Cancer. *Clinical Cancer Research* **2003,** *9*, 551–554.
4. Mehta, R.; Qureshi, M. H.; Purchal, M. K.; Greer, S. M.; Gong, S.; Ngo, C.; Que, E. L., A new probe for detecting zinc-bound carbonic anhydrase in cell lysates and cells. *Chem Commun (Camb)* **2018,** *54* (43), 5442-5445.
5. Lou, Y.; McDonald, P. C.; Oloumi, A.; Chia, S.; Ostlund, C.; Ahmadi, A.; Kyle, A.; Auf dem Keller, U.; Leung, S.; Huntsman, D.; Clarke, B.; Sutherland, B. W.; Waterhouse, D.; Bally, M.; Roskelley, C.; Overall, C. M.; Minchinton, A.; Pacchiano, F.; Carta, F.; Scozzafava, A.; Touisni, N.; Winum, J. Y.; Supuran, C. T.; Dedhar, S., Targeting tumor hypoxia: suppression of breast tumor growth and metastasis by novel carbonic anhydrase IX inhibitors. *Cancer Res* **2011,** *71* (9), 3364-76.
6. Mizukami, S.; Takikawa, R.; Sugihara, F.; Shirakawa, M.; Kikuchi, K., Dual-Function Probe to Detect Protease Activity for Fluorescence
Measurement and 19 F MRI. *Angewandte Chemie* **2009,** *121*, 3695-3697.
7. Puerta, D.; Lewis, J.; Cohen, S., New Beginnings for Matrix Metalloproteinase Inhibitors: Identification of
High-Affinity Zinc-Binding Groups. *JACS Communications* **2004,** *126*, 8388-8389.
8. Sainlos, M.; Imperiali, B., Synthesis of anhydride precursors of the environment-sensitive fluorophores 4-DMAP and 6-DMN. *Nat Protoc* **2007,** *2* (12), 3219-25.
9. Matsushita, H. M., Shin Mori, Yuki Sugihara, Fuminori; Shirakawa, M.; Yoshioka, Y.; Kikuchi, K., 19 F MRI Monitoring of Gene Expression in Living Cells
through Cell-Surface b-Lactamase Activity. *ChemBioChem* **2012,** *13*, 1579-1583.
10. Catanzaro, V. G., Concetta Menchise, Valeria Padovan, Sergio Boffa, Cinzia; Dastr, W.; Chaabane, L.; Digilio, G.; Aime, S., A R 2p /R 1p Ratiometric Procedure to Assess Matrix Metalloproteinase-2
Activity by Magnetic Resonance Imaging. *Angewandte Communications* **2013,** *52*, 3926 –3930.
11. Takaoka, Y. K., Keishi Mizusawa, Keigo Mats, Kazuya Nagasaki, Michiko; Matsuda, T.; Hamachi, I., Systematic Study of Protein Detection Mechanism of Self-Assembling
19 F NMR/MRI Nanoprobes toward Rational Design and Improved
Sensitivity. *Journal of the American Chemical Society* **2011,** *133*, 11725–11731.
12. Xie, D. K., Seyong Kohl, Vikraant Banerjee, Arnab Yu, Meng Enriquez, Jose´ Luci, Je ff rey; Que, E., Hypoxia-Responsive 19 F MRI Probes with Improved Redox Properties
and Biocompatibility. *Inorganic Chemistry* **2017,** *56*, 6429-6437.
13. Supuran, C., Carbonic anhydrase inhibitors. *Bioorganic & Medicinal Chemistry Letters* **2010,** *20*, 3467-3474.
14. Supuran, C. T.; Scozzafava, A.; Casini, A., Carbonic anhydrase inhibitors. *Med Res Rev* **2003,** *23* (2), 146-89.
15. Xie, D.; King, T. L.; Banerjee, A.; Kohl, V.; Que, E. L., Exploiting Copper Redox for 19 F Magnetic Resonance-Based
Detection of Cellular Hypoxia. *Journal of the American Chemical Society* **2016,** *138*, 2937−2940.

16. Lakowicz, J. R., *PRINCIPLES OF FLUORESCENCE SPECTROSCOPY*. 3rd ed.; Springer Science & Business Media: 2006.
17. Liu, X.; Qiao, Q.; Tian, W.; Liu, W.; Chen, J.; Lang, M. J.; Xu, Z., Aziridinyl Fluorophores Demonstrate Bright Fluorescence and Superior Photostability by Effectively Inhibiting Twisted Intramolecular Charge Transfer. *J Am Chem Soc* **2016,** *138* (22), 6960-3.
18. Soujanya, T.; Fessenden, R. W.; Samanta, A., Role of Nonfluorescent Twisted Intramolecular Charge Transfer State on the Photophysical Behavior of Aminophthalimide Dyes. *The Journal of Physical Chemistry* **1996,** *100* (9), 3507-3512.
19. Drescher, D. G., Purification of Blood Carbonic Anhydrases and Specific Detection of Carbonic Anhydrase lsoenzymes on Polyacrylamide Gels with 5Dimethylaminonaphthalene-l-Sulfonamide (DNSA) *Analytical Biochemistry* **1978,** *90*, 349-358.